Development Advance Online Articles. First posted online on 28 July 2016 as 10.1242/dev.129338
Access the most recent version at http://dev.biologists.org/lookup/doi/10.1242/dev.129338

SARA regulates neuronal migration during neocortical development through L1 trafficking

Iván Mestres[1,2], Jen-Zen Chuang[3], Federico Calegari[2], Cecilia Conde[1,4], Ching-Hwa Sung[3,5]*

[1] INIMEC, Instituto de Investigación Médica Mercedes y Martín Ferreyra, CONICET, Universidad Nacional de Córdoba UNC. Friuli 2434 - 5016 Córdoba, Argentina.

[2] DFG-Research Center for Regenerative Therapies, Cluster of Excellence, TU-Dresden, Fetscherstrasse 105, Dresden 01307, Germany.

[3] Department of Ophthalmology, Dyson Vision Research Institute, Weill Medical College of Cornell University, New York, NY 10065, USA.

[4] Instituto Universitario Ciencias Biomédicas Córdoba (IUCBC).

[5] Departments of Cell and Developmental Biology, Weill Medical College of Cornell University, New York, NY 10065, USA.

* Correspondence: chsung@med.cornell.edu

Key words: SARA, L1, endosomal trafficking, cortical neuron migration, adhesion

© 2016. Published by The Company of Biologists Ltd.

Development • Advance article

Summary

Here we describe how the early endosome protein SARA regulates the surface distribution of L1 which, in turn, affects cell adhesion and migration of cortical neurons.

Abstract

Emerging evidence suggests that endocytic trafficking of adhesion proteins plays a critical role in neuronal migration during neocortical development. However, the molecular insights of these processes remain elusive. Here we study an early endosomal protein Smad Anchor for Receptor Activation (SARA) in the developing mouse brain. SARA is enriched at the apical endfeet of radial glia of mouse neocortex. While silencing SARA did not lead to detectable neurogenic phenotypes, SARA-suppressed neurons exhibit impaired orientation and migration across the intermediate zone. Mechanistically, we show that SARA-silenced neurons exhibit increased surface expression of L1, a cell adhesion molecule. Neurons ectopically expressing L1 phenocopy the migration and orientation defects caused by SARA silencing, and display increased contact with neighboring neurites. L1 knockdown effectively rescues SARA suppression-caused phenotypes. SARA-silenced neurons eventually overcome their migration defect and enter later into the cortical plate. Nevertheless, these neurons localized at more superficial cortical layers compared to their controls counterparts. These results suggest that SARA regulates the orientation, multipolar-to-bipolar transition, and positioning of cortical neurons via modulating surface L1 expression.

Development • Advance article

INTRODUCTION

During embryonic corticogenesis, a radial glial (RG) cell divides symmetrically to produce two identical daughter RG at the ventricular zone (VZ). Alternatively, a RG divides asymmetrically to produce a RG and an intermediate basal progenitor. In turn, basal progenitors predominantly generate neurons (Taverna et al., 2014). Newborn neurons migrate radially to the cortical plate after temporally halting in the intermediate zone (IZ). These neurons mainly become projection neurons by extending axon processes tangentially across the IZ (Noctor et al., 2004). The final laminar cortical layers are formed “inside-out”. Later-born neurons migrate past the earlier-born ones, and hence, older neurons are situated deeper than younger neurons in the cerebral cortex (Hatanaka et al., 2004).

Neuron migration requires concerted establishment of the traction force by forming attachment between the leading processes (LPs) with the extracellular matrix (ECM) and/or neighboring cells as well as the detachment at the cell rear (Elias et al., 2007; Jossin and Cooper, 2011; Shieh et al., 2011). Emerging evidence showed that perturbing the components critical for endocytic trafficking (e.g., Rab5, Rab11, dynamin, clathrin) led to impaired cortical neuron migration by altering the surface distribution of adhesion molecules (e.g., N-cadherin, β1-integrin) (Shieh et al., 2011; Kawauchi et al., 2010).

L1 is a cell adhesion molecule best known for its importance in axon growth, guidance and fasciculation (Kamiguchi et al., 1998). Recent studies showed that L1 suppression also disrupts the radial locomotion of cortical neurons (Kishimoto et al., 2013). Mutations in L1 genes have been linked to hydrocephalus in several human congenital brain disorders (Kamiguchi et al., 1998; Weller and Gärtner, 2001). In vitro studies have shown that the axonal plasma membrane expression of L1 is tightly regulated by a transcytotic pathway (Wisco et al., 2003; Yap et al., 2008). However, little is known about the mechanisms underlying the surface expression of L1 in vivo and its physiological relevance during cortical development.

Smad Anchor for Receptor Activation (SARA) is an early endosomal (EE) protein that acts as a downstream effector of Rab5-mediated EE fusion (Hu et al., 2002). Like overexpression of constitutive active Rab5, overexpression of SARA also causes the enlargement of EEs (Itoh et al., 2002; Seet and Hong, 2001).

Development • Advance article

Furthermore, SARA has been shown to be involved in the vesicular trafficking of a variety of proteins including Delta, Notch, uninflatable, rhodopsin, transferrin, and Smad (Coumailleau et al., 2009; Loubéry et al., 2014; Chuang et al., 2007; Hu et al., 2002; Tsukazaki et al., 1998). A recent report revealed that SARA is unequally distributed to the two daughter cells of the zebrafish spinal cord neural precursor cells that undergo asymmetric division; and that the expression level of SARA plays a determinant role in the cell fate of the daughter cells (Kressmann et al., 2015). In the present study, we investigate the expression level and function of SARA during cortical development of the mouse brain.

Development • Advance article

RESULTS

SARA distributes equally into apically dividing cells

We employed both biochemical and immunohistochemical methods to investigate SARA expression in the developing mouse neocortex. In velocity gradient density fractions of E15 mouse embryonic brains, SARA was co-enriched with two other EE markers EEA1 and Rab5 (Fig. 1A). In E15 mouse cortical slices, SARA immunofluorescence appeared in bright puncta throughout all layers. SARA is particularly enriched in the apical endfeet of Nestin-labeled RG at the ventricle borders (Fig. 1B).

We then determined whether SARA distributes equally, or not, into the daughters of apically dividing RG. We identified mitotic cell pairs in cortical slices of brains transfected at E13.5 with GFP, by means of in utero electroporation (IUE), and exhibited characteristic condensed chromatin. Cortical slices were subjected to immunolabeling for endogenous SARA 40 hours after transfection (Fig. 1C). To determine if the symmetrical or asymmetrical modes of divisions affected SARA distribution among the two daughter cells we measure their cleavage plane angle. As expected (Haydar et al., 2003), most apically diving cells presented a vertical cleavage plane (60-90°) relative to the horizontal ventricle border (Fig. 1D). We assessed SARA fluorescence intensity in each daughter cell and a ratio was calculated between cell pairs. Endosomes positive for SARA expression segregated similarly along all the focal planes (Fig. S1, in Supplementary Information). For the three cleave plane categories $SARA^+$ EEs distributed roughly equally among the two cells with a ratio close to 1 (Fig. 1E). A similar analysis for Rab5 also points to a symmetrical distribution in apically dividing cells (Figs. 1F, G).

Development • Advance article

SARA in mammalian neurogenesis

To investigate the function of SARA in RG, we performed loss-of-function analysis by delivering a plasmid encoding both SARA short hairpin RNA (sh) and GFP into E13.5 cortex. Scrambled sh (Ctrolsh) was used for controls. The knockdown (KD) effect in SARAsh was previously validated (Chuang et al., 2007; Arias et al., 2015) and confirmed by SARA immunohistochemistry in transfected cortical slices (Fig. S2A).

The distribution patterns of cells transfected with Ctrolsh or SARAsh were comparable in brains harvested 40 hours after electroporation (Fig. 2A). To further test whether SARA plays a role in neurogenesis, we performed a cell cycle exit analysis. A single-pulse of BrdU was given to mice 24 hours after IUE, and the brain slices harvested 24 hours afterwards were immunolabelled for Ki67 and BrdU (Figs. 2 C, D). The cell cycle exit index was similar between cells transfected either with Ctrolsh or SARAsh (Fig. 2 B).

Furthermore, SARAsh transfection did not affect the expression pattern or number of Pax6-labeled apical progenitors and Tbr2-labeled basal progenitors (Figs. 2E, F, I, J). The fraction of mitotic Ctrolsh and SARAsh transfected cells (i.e., phospho-histone 3-positive) were indistinguishable (Figs.1G, K). Similarly to Ctrolsh transfected brain slices, the expression of SARAsh did not altered the organization of RG processes as revealed with Nestin immunostaining (Fig. S2B). Finally, SARAsh transfected cells were able to reach the IZ and display the neuron marker Tuj1 to a similar extent as the control cells (Figs. 2H, L, S2C). The data deduced from our KD experiments suggest that SARA is dispensable for the proliferation and differentiation of RG progenitors.

SARA suppression leads to neuronal migration delay in the IZ

We next examined brains 3 days after transfection and found that the large majority of control neurons (>60%) have migrated into the CP (Figs. 3A, D). By contrast, only ~14% of SARA-suppressed neurons have migrated into the CP, instead, a significant higher fraction (~75%) of them remained in the IZ (Figs. 3B, D).

Development • Advance article

Increased apoptosis is unlikely to explain the reduced number of SARA-silenced neurons at the CP because the number of cells expressing cleaved PARP (Figs. S3A, B), a main target of active caspase-3 (Tewari et al., 1995), was similar in the control and SARAsh transfected brains.

At this developmental stage, the large majority (~74%) of control neurons, either in the IZ or CP, already developed a bipolar morphology with a pia-directed LP. The orientation of the LPs was mostly between 75° and 90° relative to the ventricle border (Figs. 3A, E, H). In contrast, most SARAsh transfected neurons in the IZ were tilted; ~30% of them angled 0°-20°, and ~50% of them angled 20°-45° (Figs. 3B, arrowheads in box 2 of 3F, 3H). Whilst ~6% of SARA-suppressed neurons developed a vertical angle, both the LPs and trailing processes of these neurons were abnormally curved and branched (Figs. 3B, arrows in box1 of 3F, 3I, J).

To rule out off-target effects caused by SARAsh, we show that cells transfected with a rescue plasmid SARAsh/SARA* (encoding SARA-shRNA, sh-resistant SARA cDNA and GFP) were able to reach the CP and displayed rather normal looking, pia-oriented LPs (Fig. 3C, D, G). These results suggest that the SARA-silencing mediated phenotypes are specific.

The migration defect of SARA-suppressed neurons was unlikely to be due to a defective polarity. This is supported by the finding that the large majority (~90%) of SARAsh transfected cells had their γ-tubulin-labeled centrosome normally localized between the nucleus and the LP, indicating a rather intact internal polarity (Fig. S3C).

SARA silencing increases surface L1 and affects cell adhesion

Previous studies showed that L1-KD neurons also exhibited migration defects (Kishimoto et al., 2013) similarly to SARA-KD neurons. In E16.5 mouse cortex, L1 was abundantly expressed on the axonal tracks tangentially distributed along the IZ (Fig. 4A), as expected (Fushiki and Sachner, 1986; Chung et al., 1991). Weak L1

Development • Advance article

signal was also detected in the CP and MZ, and little or no L1 was detectable in the VZ and SVZ.

Furthermore, we show that L1 signals were frequently associated with SARA-labeled endosomes in dissociated cortical neurons (Fig. 4B), indicating that L1 is trafficked through SARA-expressing EEs. Consistent with this notion, surface distribution of L1 in axons was increased in SARA-KD neuronal cultures (Arias et al., 2015). Thus, we hypothesized that SARA silencing-induced neuronal migration defect could be related to changes in the surface expression of L1. To this end, we labeled endogenous surface L1 of neurons isolated from transfected brains. In these experiments, an antibody that specifically recognized the extracellular domain of L1 was used to stain under the non-permeabilizing conditions. Notably, surface L1 was predominantly expressed in a single process (likely the future axon) of GFP transfected neurons (arrows in Fig. 4C, top panel). In contrast, detectably increased L1 was found on almost all processes of SARA-sh transfected neurons (arrows in Fig. 4C, middle panel). Quantification studies showed that SARAsh-transfected neurons had ~3.5 fold more L1 displayed on the plasma membrane of neuronal processes compared to the control GFP-transfected neurons (Fig. 4D). By contrast, we showed that the surface expression of β1-integrin in SARA-KD neurons was unchanged compared to controls (Figs. S4A, B).

To evaluate whether surface L1 increase affects cell adhesion, we examined the cortical cells dissociated from brain cortices 2 days after transfection and cultured for additional 2 days. We used Nestin and doublecortin (DCX) to label progenitor cells and neurons, respectively. We found that neuronal processes extended from control neurons preferentially contacted Nestin+ progenitor cells rather than DCX+ neurons (Fig. 4E, F, S4C). Contrarily, SARAsh transfected neurons preferentially contacted other DCX+ neurons, rather than Nestin+ progenitor cells.

Development • Advance article

L1 suppression rescues the phenotypes caused by SARA silencing

The above results prompted us to hypothesize that the impaired IZ exit of SARA-suppressed migrating neurons is due to elevated L1 surface expression. Consistent with this model, we show that in 3-days transfected brains the majority of neurons overexpressing L1-YFP also failed to reach the CP and were retained in the IZ (Fig. 5A, C). These neurons were horizontally or obliquely aligned similarly to the SARA-suppressed neurons (Fig. 5B, D).

Resembling SARAsh transfected neurons, the surface L1 signal was similarly increased in multiple processes of L1-YFP expressing neurons isolated from transfected brains (Fig. 4C, D). Consistently, the ectopically expressed L1-YFP was also prominently detected in the LPs of migrating neurons (arrows, Fig. 5B). 3D rendering of confocal images showed that both the soma and processes of L1-YFP overexpressing neurons in the IZ had multiple contacts with the processes extended by other transfected neurons (Fig. 5B, E, F, and Movie 1), indicating that increased cell-cell contact in these neurons is a result of increased surface L1.

Next, we addressed whether upregulated L1 expression is accountable for SARA-silencing mediated phenotypes. To this end, we generated an L1sh plasmid and validated its KD effect by immunoblotting of co-transfected L1-YFP cell lines (up to ~40% of control; Fig. 5G). Similarly to previous studies (Kishimoto et al., 2013), neurons transfected for three days with our L1sh construct led to migration arrest around the IZ (Figs. S5A, B). Finally, three-day transfected neurons co-expressing SARAsh and L1sh displayed a vertical orientation and ~60% of them reached the CP similarly to Ctrolsh transfected neurons (Fig. 5H, I). These results suggest that SARA-silencing caused phenotypes can be effectively rescued by simultaneous silencing of L1.

Development • Advance article

SARA is required for neuronal multipolar to bipolar transition

To further delineate the mechanism underlying SARA-KD mediated neuronal migration defect, we imaged transfected neurons on live brain slices for 12-14 hours. As expected (Noctor et al., 2004), multipolar Ctrolsh transfected neurons exited the IZ, acquired a bipolar morphology with a pia-directed leading process and migrated towards the CP (Figs. 6A, C, Movie 2). Conversely, neurons expressing SARAsh exhibited characteristic multipolar dynamics throughout the recording. These neurons constantly extended and retracted their neuronal processes in various directions, and frequently changed orientation (Figs. 6B, C, Movie 3). Almost no SARAsh transfected cell was able to exit the IZ during the 14 hours imaging period. Furthermore, the migration speed of transfected neurons was also significantly slower in SARAsh expressing cells compared to their control counterparts (Fig. 6D).

SARA-KD neurons arrive late into the CP

By examining 5-day transfected brains, we found that both Ctrolsh and SARAsh transfected neurons were able to reach the CP with their LPs contacting the MZ (Figs. 7A-C). Immunolabeling of SARAsh transfected neurons showed that the silencing effect remained valid at this time point (Figs. S6A, B). Thus, these results indicate that the delayed IZ exit of SARAsh-transfected neurons was overcome with time. Consistent with a retarded migration through the IZ, SARA-suppressed neurons were localized in the more superficial cortical layers relatively to the Ctrolsh transfected neurons (Figs. 7B, C). In addition, SARA-suppressed neurons tended to cluster together presumably due to the stronger adhesion.

Notably, the LPs of both control and SARA-suppressed neurons reached the MZ (Figs. 7D, E). Despite their similarity in length (Fig. 7F), the LPs of SARAsh transfected neurons exhibited a greater curvature compared to those of the controls (Figs. 7D, E). The curvilinear index (Fig. 7G) indicated that this morphological difference is statistically significant. These results suggest that SARA is important for a timely migration and positioning into the CP and for the LP morphogenesis of cortical projection neurons.

Development • Advance article

SARA silenced neurons distribute to superficial layers in the postnatal cortex

We next evaluated whether the delayed migration in SARA-KD neurons affected the later corticogenesis. To this end, we studied transfected brains at postnatal day (P) 15, when neuronal migration is largely completed (Molyneaux et al., 2007). At this time point, SARA-KD neurons were distributed to the more superficial layers compared to control neurons (Figs. 8A, B). Using layer-specific makers, we found that ~70% of Ctrolsh-expressing cells localized to the deep (i.e., V and VI) layers that expressed Ctip2, whereas a minor fraction expressed the upper-layers marker Cux1 (layers II-IV) (Fig. 8C). By contrast, the large majority of SARA-KD neurons were mapped to Cux1+ layers II-IV. Consistently, compared to the controls, the fraction of SARA-KD neurons positive for Ctip2 and Cux1 decreased and increased, respectively (Fig. 8D). At this age (P15) we did not detect any major differences in apical dendrite morphology between Ctrolsh and SARAsh transfected cells (not shown).

These data support the idea that SARA-KD caused migration defects affect the laminar cortical layer development in the postnatal brain.

Development • Advance article

DISCUSSION

SARA is dispensable for the mitosis and neurogenesis of mammalian RG

Previous studies showed that SARA-expressing EEs play an important role in determining the asymmetric cell division in Drosophila sensory organ precursor cells (SOP) via modulating the Notch-Delta signaling (Coumailleau et al., 2009). However, SARA itself is dispensable for the asymmetric segregation of Delta and Notch and SOP development. Subsequent studies showed that in dividing cells of the zebrafish spinal cord SARA segregated asymmetrically, but Rab5 distributed symmetrically. In this model, the daughter cells that inherited more SARA-expressing EEs remain as proliferative progenitors through a Notch dependent pathway, whereas the daughter cells containing less SARA-expressing EEs tended to leave cell cycle and differentiate into neurons (Kressmann et al. 2015).

Here we show that in the E15 mouse cortex SARA, as well as Rab5, is roughly equally distributed in the two daughters of a dividing RG. Furthermore, the expression pattern of specific markers for neuron, apical progenitor, basal progenitor, and mitotic cells are comparable between SARAsh and control transfected brains. Progenitor cell cycle exit also is unaffected after SARA KD. Thus, our results suggest that SARA is not critical for the mitosis and cell fate determination of RG in the developing mouse neocortex. This finding is unexpected given that SARA is enriched in RG apical endfeet, and that Notch is critical for the asymmetric cell division of rodent RG (Bultje et al., 2009). We cannot completely exclude the possibility that residual SARA in the SARAsh-transfected apical progenitors obscured our detection of its role in neurogenesis. However, we prefer a model whereby a redundant endocytic pathway is used to compensate for Notch-mediated asymmetric division when SARA is silenced in the mammalian neocortex. SARA is a FYVE (Fab1p, YOTB, Vac1p, and EEA1) domain-containing protein. Several FYVE domain-containing proteins, such as EEA1 and Hrs, are also enriched in EEs and have been involved in endocytic vesicular trafficking (Stenmark and Aasland, 1999; Panopoulou et al., 2002) (see below).

Development • Advance article

SARA regulates multipolar to bipolar transition and CP positioning

Both the cell distribution and live imaging studies showed that SARA suppression causes a prominent delay in the migration of post-mitotic neurons through the IZ. Increased surface expression of L1 likely contributes to this phenotype because: (1) SARA-KD neurons are stalled at the IZ, a region in which L1 is highly expressed (Fushiki & Schachner, 1986; Chung et al, 1991), (2) overexpression of L1 phenocopies SARA KD mediated phenotypes, and most importantly, (3) L1 suppression can rescue SARA KD mediated defects.

The surface expression level of L1 appears to be tightly regulated during neuronal development: neurons expressing either too little (Kishimoto et al., 2013; Demyanenko et al., 1999) or too much (this paper) L1 exhibit impaired migration and morphology/orientation of their LPs. Weakened adhesions may fail to provide sufficient traction force for forward movement, whereas excessive adhesions cause cell (and/or cell processes) to stick to each other and/or ECM, preventing their detachment (Shikanai et al., 2011). While L1 is typically enriched on the axonal surface of WT neurons (Fig. 9A), it is increasingly expressed on all processes of SARA-KD or L1-YFP overexpressing neurons (Fig. 9B). We showed that SARA-silenced neurons preferentially adhere to other neurons at the expense of their adhesion to progenitor cells. The increased L1 in LPs of migrating neurons in vivo may enable a preferred binding with neurites of other IZ-localized neurons and/or axonal processes of CP neurons. L1 is a transmembrane protein with extracellular immunoglobulin-like and fibronectin III domains. It may interact with L1 molecules (trans-homophilic interaction) or other adhesion molecules such as: axonin-1, integrins, and phosphacan (trans-heterophilic interaction) (Kuhn et al., 1991; Yip and Siu, 2001; Milev et al., 1994). Alternatively, L1 can also bind to the ECM. Enhanced adhesion may explain the abnormal orientation of mutant neurons and their reduced migration towards the CP (Fig. 9B).

The multipolar-to-bipolar transition is an important step before engaging in radial glia-guided migration. Namely, multipolar cells in the upper SVZ and lower IZ need to acquire a bipolar morphology in which a stable pia-directed LP heads the migration out of the IZ and into the CP (Kriegstein and Noctor, 2004, LoTurco and Bai, 2006). Our time-lapse experiments revealed that the multipolar-to-bipolar

Development • Advance article

transition is largely impaired after SARA KD. These neurons consistently drifted randomly at the IZ and exhibited numerous highly dynamic neurites.

The SARA-silencing induced radial migration defect was partially overcome with time. In line with the idea that SARA-suppressed neurons arrive later to the CP, their somata resided in more upper cortical layers relatively to control neurons.

SARA regulates the surface expression of L1

While the importance of cytoskeletal and motor proteins (e.g., filamin, LIS1, DCX, RhoA, myosin II, dynein) in neocortical development has been extensively established (Nagano et al., 2004; Tsai et al., 2005, 2007; Bai et al., 2003; Cappello et al., 2012; Solecki et al., 2009), only until recently, evidence began to emerge indicating that the endosomal trafficking also participates in guided neuron migration and proper positioning (Shieh et al., 2011; Kawauchi et al., 2010; Zhou et al., 2007). It has been well established that internalized surface molecules can be either transported back to the plasma membrane from the EEs via a “fast-recycling pathway”, or through Rab11+ recycling endosomes via a “slow-recycling pathway” (Maxfield and McGraw, 2004). It is well known that transferrin and its receptor are trafficked through the slow recycling pathway. SARA has been previously shown to regulate transferrin’s recycling; overexpression of SARA significantly delays the recycling of transferrin as well as transferrin receptor (Hu et al., 2002). However, the level of SARA is not critical for the internalization rate of transferrin.

In cortical neurons, L1 has been shown to be transcytosed from the somatodendritic domain to the axonal plasma membrane through the slow recycling pathway (Wisco et al., 2003). Our unpublished data show that recycling endosome genesis requires SARA (Hus, Chuang, Sung, in preparation). Thus, L1 may be shifted to the fast-recycling pathway in SARA-suppressed cells. This may explain its overall increased surface expression. Since only a trace amount of internalized L1 (~10%) undergoes lysosomal degradation (Schäffer et al., 2010), it is less likely that deregulated degradation levels accounts for the increased L1 surface expression in SARA-KD cells.

Development • Advance article

Consistent with SARA's role in Rab5-mediated EE fusion (Hu et al., 2002), SARA-KD neurons exhibit branched LPs and migration defects similar to those observed after Rab5 KD (Kawauchi et al., 2010). Rab5 KD mediated phenotypes rely on elevated surface expression of N-Cadherin. While we do not know whether SARA KD also affects N-Cadherin expression, the surface β1-intergrin expression was unchanged in SARA-KD neurons. This indicates that L1 increase in SARA-KD neuron is selective. Our other data suggest that SARA-KD mediated phenotypes can be accountable by the increase of L1. Importantly, elevated L1 expression also explains the neuronal alignment defects observed in SARA KD, but not in Rab5 KD (Kawauchi et al., 2010).

In addition to SARA, coincidently, several proteins also known to be involved in Rab5-mediated EE fusion (e.g., Rabex-5, EHD1/EHD4, EEA1) have been implied in L1 surface recycling (Aikawama, 2012; Yap et al., 2010; Lasiecka et al., 2014). For example, the surface expression of L1 is increased in dendrites of EHD1-overexpressing neurons (Yap et al., 2010). Similar to our current finding, a compensatory mechanism emerges later to alleviate this defect. This redundancy of trafficking regulation reiterates the importance of tight control of L1 surface expression level. Notably, L1 is upregulated in post-stroke cortex and has been implicated in axonal regeneration after spinal cord injury (Carmichael et al., 2005; Roonprapunt et al., 2003; Chen et al., 2007). Thus, our finding that SARA regulates the surface expression level of L1 in the cerebral cortex in vivo might be clinically relevant.

Finally, while highly controversial (Bakkebo et al., 2012; Runyan et al., 2012), SARA has been reported to be important for the activation of transformation growth factor beta (TGFβ) signaling pathway (Tsukazaki et al., 1998; Itoh et al., 2002); whether this functional aspect of SARA plays a role in L1 surface expression remains to be investigated.

Development • Advance article

MATERIALS AND METHODS

The information of Regents and Image Quantitative Analyses is included in Supplementary Materials

Velocity density gradient sedimentation, protein electrophoresis, and immunoblotting assays

Protocol was conducted as previously described (Sachdev et al., 2007). Embryonic E15.5 mouse brains were harvested and homogenized. The high-speed supernatant fraction was fractionated in a 5–20% linear sucrose gradient in 11 ml of Tris–KCl buffer (20mM Tris, pH 7.5, 50mM KCl, 5mM MgCl2, 0.5mM EGTA, 0.5mM DTT, and protease inhibitors) at 32 000 rpm in 4°C for 16 h. Equal amount of each fraction was subjected to immunoblotting assays using standard method.

IUE, brain tissue processing and neuron culture

IUE procedures were performed on E13.5 mouse brains as previously described (Li et al., 2011; Artegiani et al., 2012). Briefly, the embryonic ventricles were injected with a mixture of plasmids (2µg/µl), fast green dye and TE buffer. Immediately, three square electric pulses (30V) were delivered using a BTX electroporator (Harvard Apparatus). All embryos were placed back to their original position and sutured. Female mice were allowed to recover from anesthesia on a warm plate.

For cell cycle exit analysis, pregnant mice (20-30g) were injected with 1mg BrdU 24 h after IUE, and fetal brains were harvested 24 h after BrdU treatment. Electroporated brains were harvested at the indicated time points. Embryonic brains were fixed by immersion with 4% paraformaldehyde and 0.0125% glutaraldehyde overnight at 4°C, while postnatal animals were transcardially perfused with 4% paraformaldehyde and their brains were postfixed by immersion in the same fixative. Brains were embedded in low melting agarose, and sectioned by vibratome (40 µm thick). All animal manipulations were performed in accordance with the guidelines for animal experiments at Weill Medical Cornell IACUC, at Instituto M. y M. Ferreyra CICUAL, and Landesdirektion Sachsen.

In some experiments, electroporated brain cortices were dissociated with trypsin, dispersed on poly-L-lysine coated coverslips and incubated at 37°C in Neurobasal (GIBCO) supplemented with B27, N2 and Glutamax (GIBCO). For co-

Development • Advance article

culture of primary cortical neurons with Nestin+ cells, medium consisted in Neurobasal supplemented with 10% horse serum. At the indicated time points (2 or 5 days after seeding) cells were fixed with 4% paraformaldehyde and 4% sucrose in PBS followed by immunolabeling using standard protocol. Surface L1 or β1-integrin labeling was conducted similarly except Triton X-100 was omitted during the incubation with the primary and secondary antibodies. Cells were then permeabilized with 0.2% Triton X-100 before cytoskeleton counterstaining.

Slice culture and time-lapse imaging

Brains were harvested 2 days after electroporation (E15.5), and embedded in low melting point agarose at 37°C. The tissue was immediately sliced at 250µm with a vibratome. Brain sections were transferred to membrane inserts for 6-well culture plates (BD Falcon), preincubated with 1.5ml culture media containing Neurobasal (GIBCO) supplemented with 10% horse serum and antibiotics. The tissue was allowed to recover and to attach to the insert for 2 hours before imaging.

Time-lapse imaging was performed with an inverted confocal microscope (Zeiss LSM 780) using a Plan-Apochromat 10X air objective (NA 0.45) with a temperature-controlled incubator (Life Imaging Services) and CO_2 set to 5% (Pecon). Stacks were captured every 30 min for 12hr. The migrating neurons were tracked and analyzed with the Manual Tracking plugin in ImageJ. At least six slices from three independent experiments were analyzed for each condition.

Acknowledgements

We thank the light microscopy facility of the BIOTEC/CRTD for excellent support. We also thank H. Kamiguchi (RIKEN, Japan) and D. Carrer (INIMEC-CONICET, Argentina) for reagents; M. Lorenzatti for assistance with Figure 9; and A. Caceres for discussion.

Competing interests

The authors declare no competing financial interests.

Author contributions

IM performed experiments, data analysis and prepared manuscript; J-Z C designed reagents and experiments; CC and FC shared unpublished reagents; C-H S developed concepts, design experiments, performed data analysis, and prepared manuscript.

Funding

This work was supported by NIH NEI (EY11307 and EY016805), Starr Foundation, and Research to Prevent Blindness to C-H. S. Travel grants from Journal of Cell Science and International Society for Neurochemistry, and a CONICET fellowship were awarded to I.M. CRTD, TUD and DFG Collaborative Research Center SFB655 (subproject A20) supported F.C. PICT 2008-0671 was granted to C.C.

Development • Advance article

References

Aikawa Y. (2012). Rabex-5 Protein Regulates the Endocytic Trafficking Pathway of Ubiquitinated Neural Cell Adhesion Molecule L1. J. Biol. Chem. **287**(39), 32312-32323.

Arias C. I., Siri S. O., Conde C. (2015). Involvement of SARA in Axon and Dendrite Growth. PLoS ONE **10**(9): e0138792.

Artegiani B., Lange C., Calegari F. (2012) Expansion of embryonic and adult neural stem cells by in utero electroporation or viral stereotaxic injection. J Vis Exp e4093. doi: 10.3791/4093

Bai J., Ramos R. L., Ackman J. B., Thomas A. M., Lee R. V., LoTurco J. J. (2003). RNAi reveals doublecortin is required for radial migration in rat neocortex. Nat. Neurosci. **6**(12), 1277-1283.

Bakkebø M., Huse K., Hilden V. I., Forfang L., Myklebust J. H., Smeland E. B., Oksvold M. P. (2012). SARA is dispensable for functional TGF-β signaling. FEBS Lett. **586**(19), 3367-3672.

Bultje R. S., Castaneda-Castellanos D. R., Jan L. Y., Jan Y. N., Kriegstein A. R. (2009). Mammalian Par3 regulates progenitor cell asymmetric division via notch signaling in the developing neocortex. Neuron **63**(2), 189-202.

Carmichael S. T., Archibeque I., Luke L., Nolan T., Momiy J., Li S. (2005). Growth-associated gene expression after stroke: Evidence for a growth-promoting region in peri-infarct cortex. Exp. Neu. **193**(2), 291-311.

Cappello S., Böhringer C. R. J., Bergami M., Conzelmann K.-K., Ghanem A., Tomassy G. S., Arlotta P., Mainardi M., Allegra M., Caleo M., van Hengel J., Brakebusch C., Götz M. (2012). A radial glia-specific role of RhoA in double cortex formation. Neuron **73**(5), 911-924.

Chen J., Wu J., Apostolova I., Skup M., Irintchev A., Kügler S., Schachner M. (2007). Adeno-associated virus-mediated L1 expression promotes functional recovery after spinal cord injury. Brain **130**(4), 954-969.

Development • Advance article

Chuang J. Z., Zhao Y., Sung C.-H. (2007). SARA-regulated vesicular targeting underlies formation of the light-sensing organelle in mammalian rods. Cell **130**, 1-13.

Chung W. W., Lagenaur C. F., Yan Y. M., Lund J. S. (1991). Developmental expression of neural cell adhesion molecules in the mouse neocortex and olfactory bulb. J. Comp. Neurology **314**(2), 290-305.

Coumailleau F., Fürthauer M., Knoblich J.A., González-Gaitán M. (2009). Directional Delta and Notch trafficking in Sara endosomes during asymmetric cell division. Nature **458**(7241), 1051-1055.

Demyanenko G., Tsai A., Maness P. (1999). Abnormalities in neuronal process extension, hippocampal development, and the ventricular system of L1 knockout mice. J. Neurosci. **19**, 4907–4920.

Elias L. A., Wang D. D., Kriegstein A. R. (2007). Gap junction adhesion is necessary for radial migration in the neocortex. Nature. **448**, 901–907.

Fushiki S. and Schachner M. (1986). Immunocytological localization of cell adhesion molecules L1 and N-CAM and the shared carbohydrate epitope L2 during development of the mouse neocortex. Dev. Brain Res. **24**, 153-167.

Hatanaka Y., Hisanaga S. I., Heizmann C. W., Murakami F. (2004). Distinct migratory behavior of early- and late-born neurons derived from the cortical ventricular zone. J. Comp. Neuro. **479**, 1-14.

Hu Y., Chuang J.-Z., Xu K., McGraw T., Sung C.-H. (2002). SARA, a FYVE domain protein, affects Rab5-mediated endocytosis. J. Cell Science **115**(24), 4755-4763.

Itoh F., Divecha N., Brocks L., Oomen L., Janssen H., Calafat J., Itoh S., Dijke P. P. (2002). The FYVE domain in Smad anchor for receptor activation (SARA) is sufficient for localization of SARA in early endosomes and regulates TGF-beta/Smad signaling. Genes Cells **7**, 321-331.

Jossin Y. and Cooper J. A. (2011). Reelin, Rap1 and N-cadherin orient the migration of multipolar neurons in the developing neocortex. Nat. Neurosci. **14**, 697–703.

Development • Advance article

Kamiguchi H., Hlavin M. L., Lemmon V. (1998). Role of L1 in neural development: what the knockouts tell us. Mol. Cell. Neurosci. **12**, 48-55.

Kawauchi T., Sekine K., Shikanai M., Chihama K., Tomita K., Kubo, K.-i., Nakajima K., Nabeshima, Y.-I., Hoshino M. (2010). Rab GTPases-dependent endocytic pathways regulate neuronal migration and maturation through N-cadherin trafficking. Neuron **67**, 588-602.

Kishimoto T., Itoh K., Umekage M., Tonosaki M., Yaoi T., Fukui K., Lemmon V. P., Fushiki S. (2013). Downregulation of L1 perturbs neuronal migration and alters the expression of transcription factors in murine neocortex. J. Neu. Res. **91**, 42-50.

Kressmann S., Campos C., Castanon I., Fürthauer M., González-Gaitán M. (2015). Directional Notch trafficking in Sara endosomes during asymmetric cell division in the spinal cord. Nat. Cell Biol. **17**(3), 333-339.

Kriegstein, A. R., Noctor, S. C. (2004). Patterns of neuronal migration in the embryonic cortex. Trends in neurosciences **27**(7), 392-399.

Kuhn T. B., Stoeckli E. T., Condrau M. A., Rathjen F. G., Sonderegger P. (1991). Neurite outgrowth on immobilized axonin-1 is mediated by a heterophilic interaction with L1(G4). J. Cell Biol. **115**(4), 1113-1126.

Lasiecka Z. M., Yap C. C., Katz J., Winckler B. (2014). Maturational conversion of dendritic early endosomes and their roles in L1-mediated axon growth. J Neurosci. **34**(44), 14633-14643.

Li A., Saito M., Chuang J.-Z., Tseng Y.-Y., Dedesma C., Tomizawa K., Kaitsuka T., Sung C.-H. (2011). Ciliary transition zone activation of phosphorylated Tctex-1 controls ciliary resorption, S-phase entry and fate of neural progenitors. Nature Cell Bio. **13**(4), 402-411.

Loubéry S., Seum C., Moraleda A., Daeden A., Fürthauer M., Gonzalez-Gaitan M. (2014). Uninflatable and Notch control the targeting of sara endosomes during asymmetric division. Curr. Biol. **24**(18), 2142-2148.

LoTurco, J. J., Bai, J. (2006). The multipolar stage and disruptions in neuronal migration. Trends in neurosciences **29**(7), 407-413.

Development • Advance article

Maxfield F. R and McGraw T. E. (2004). Endocytic recycling. Nat. Rev. Mol. Cell. Bio. **5**, 121-132.

Milev P., Friedlander D. R., Sakurai T., Karthikeyan L., Flad M., Margolis R. K., Grumet M., Margolis R. U. (1994). Interactions of the chondroitin sulfate proteoglycan phosphacan, the extracellular domain of a receptor-type protein tyrosine phosphatase, with neurons, glia, and neural cell adhesion molecules. J. Cell Biol. **127**, 1703–1715.

Molyneaux, B. J., Arlotta, P., Menezes, J. R. L., Macklis, J. D. (2007). Neuronal subtype specification in the cerebral cortex. Nat. Rev. Neurosc. **8**(6), 427-437.

Nagano T., Morikubo S., Sato M. (2004). Filamin A and FILIP (Filamin A-Interacting Protein) regulate cell polarity and motility in neo- cortical subventricular and intermediate zones during radial migration. J. Neurosci. **24**, 9648–9657.

Nishimura K., Yoshihara F., Tojima T., Ooashi N., Yoon W., Mikoshiba K., Bennett V., Kamiguchi H. (2003). L1-dependent neuritogenesis involves ankyrinB that mediates L1-CAM coupling with retrograde actin flow. J. Cell Biol. **163**(5), 1077-1088.

Noctor, S. C., Martínez-Cerdeño, V., Ivic, L., Kriegstein, A. R. (2004). Cortical neurons arise in symmetric and asymmetric division zones and migrate through specific phases. Nature neuroscience **7**(2), 136-144.

Panopoulou E., Gillooly D. J., Wrana J. L., Zerial M., Stenmark H., Murphy C., Fotsis T. (2002). Early endosomal regulation of Smad- dependent signaling in endothelial cells. J. Biol. Chem. **277**, 18046-18052.

Roonprapunt C., Huang W., Grill R., Friedlander D., Grumet M., Chen S., Schachner M., Young W. (2003). Soluble cell adhesion molecule L1-Fc promotes locomotor recovery in rats after spinal cord injury. J. Neurotrauma **20**(9), 871-882.

Runyan C. E., Liu Z., Schnaper H. W. (2012). Phosphatidylinositol 3-kinase and Rab5 GTPase inversely regulate the Smad anchor for receptor activation (SARA) protein independently of transforming growth factor-β1. J. Biol. Chem. **287**, 35815-35824.

Development • Advance article

Sachdev P., Menon S., Kastner D., Chuang, J.-Z., Yeh T.-Y., Caceres A., Sung C.-H., Sakmar T. P. (2007). G protein βγ subunit interaction with the dynein light chain component Tctex-1 regulates neurite outgrowth. The EMBO Journal **26**, 2621-2632.

Schäfer M. K., Schmitz B., Diestel S. (2010). L1CAM ubiquitination facilitates its lysosomal degradation. FEBBS letters **584**, 4475-4480.

Seet, L. F. and Hong, W. (2001). Endofin, an endosomal FYVE domain protein. J. Biol. Chem. **276**, 42445–42454.

Shieh J., Schaar B., Srinivasan K., Brodsky F., McConnell S. (2011). Endocytosis regulates cell soma translocation and the distribution of adhesion proteins in migrating neurons. PLoS ONE **6**, e17802.

Shikanai M., Nakajima K., Kawauchi T. (2011). N-cadherin regulates radial glial fiber-dependent migration of cortical locomoting neurons. Commun. Integr. Biol. **4**(3), 326-330.

Solecki D. J., Trivedi N., Govek E.-E., Kerekes R. A., Gleason S. S., Hatten M. E. (2009). Myosin II motors and F-actin dynamics drive the coordinated movement of the centrosome and soma during CNS glial-guided neuronal migration. Neuron **63**(1), 63-80.

Stenmark H. and Aasland R. (1999). FYVE-finger proteins-effectors of an inositol lipid. J Cell Sci. **112**, 4175-4183.

Taverna E., Gotz M., Huttner W.B. (2014). The cell biology of neurogenesis: toward an understanding of the development and evolution of the neocortex. Annu. Rev. Cell Dev.
Biol. **30**, 465–502.

Tewari M., Quan L. T., O'Rourke K., Desnoyers S., Zeng Z., Beidler D. R., Poirier G. G., Salvesen G. S., Dixit V. M. (1995). Yama/CPP32 beta, a mammalian homolog of CED-3, is a CrmA-inhibitable protease that cleaves the death substrate poly(ADP-ribose) polymerase. Cell **81**(5), 801-809.

Development • Advance article

Tsai J.-W., Chen Y., Kriegstein A. R., Vallee R. B. (2005). LIS1 RNA interference blocks neural stem cell division, morphogenesis, and motility at multiple stages. J. Cell Bio. **170**(6), 935-945.

Tsai J.-W., Bremner K. H., Vallee R. B. (2007). Dual subcellular roles for LIS1 and dynein in radial neuronal migration in live brain tissue. Nat. Neurosci. **10**, 970–979.

Tsukazaki T., Chiang T. A., Davison A. F., Attisano L., Wrana J. L. (1998). SARA, a FYVE domain protein that recruits Smad2 to the TGFbeta receptor. Cell **95**, 779–791.

Weller S. and Gärtner J. (2001). Genetic and clinical aspects of X-linked hydrocephalus (L1 disease): Mutations in the L1CAM gene. Hum. Mutat. **18**(1), 1-12.

Wisco D., Anderson E. D., Chang M. C., Norden C., Boiko T., Fölsch H., Winckler B. (2003). Uncovering multiple axonal targeting pathways in hippocampal neurons. J. Cell Bio. **162**(7), 1317-1328.

Yap C. C., Wisco D., Kujala P., Lasiecka Z. M., Cannon J. T., Chang M. C., Hirling H., Klumperman J., Winckler B. (2008). The somatodendritic endosomal regulator NEEP21 facilitates axonal targeting of L1/NgCAM. J. Cell Bio. **180**(4), 827-842.

Yap C. C., Lasiecka, Z. M., Caplan S., Winckler B. (2010). Alterations of EHD1/EHD4 Protein Levels Interfere with L1/NgCAM Endocytosis in Neurons and Disrupt Axonal Targeting. J. Neurosci. **30**(19), 6646-6657.

Yip P. M. and Siu C. H. (2001). PC12 cells utilize the homophilic binding site of L1 for cell-cell adhesion but L1-alphavbeta3 interaction for neurite outgrowth. J. Neurochem. **76**(5), 1552-1564.

Zhou P., Porcionatto M., Pilapil M., Chen Y., Choi Y., Tolias K. F., Bikoff J. B., Hong E. J., Greenberg M. E., Segal R. A. (2007). Polarized signaling endosomes coordinate BDNF-induced chemotaxis of cerebellar precursors. Neuron **55**, 53-68.

Development • Advance article

Figures

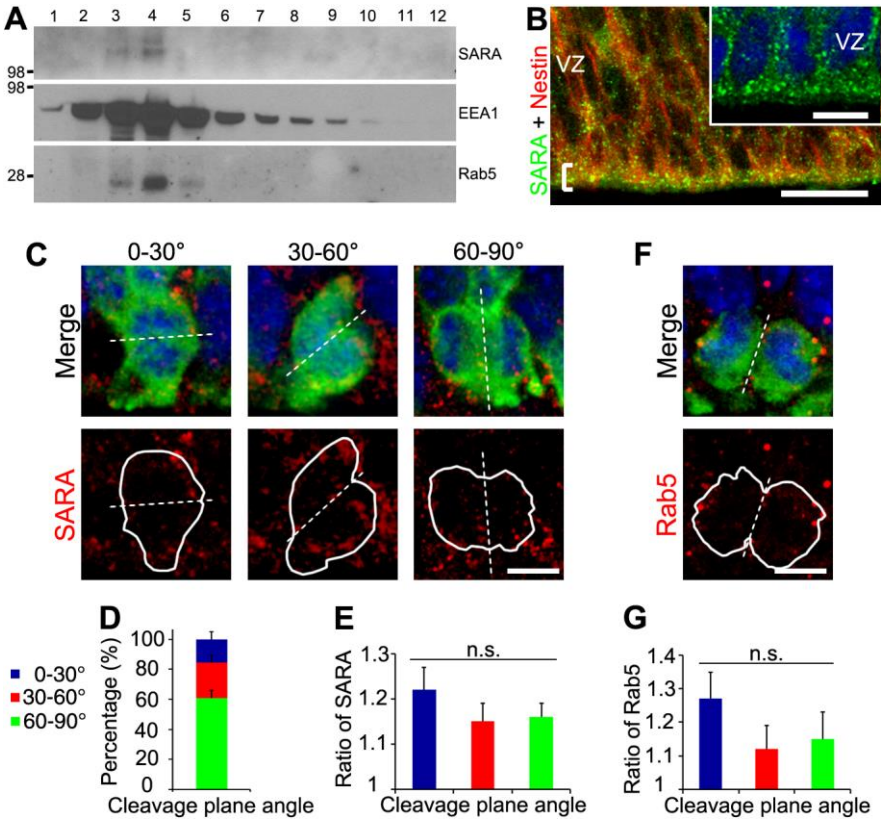

Figure 1. The expression pattern of EE protein SARA in developing neocortex and its distribution in dividing apical progenitors. (A) E15.5 mouse brains were homogenized and sedimented in a 5–20% linear sucrose gradient. Equal amount of each fraction was immunoblotted with the indicated antibodies. (B) Confocal images of the ventricular surface of E15.5 mouse neocortical slices double labeled with SARA and Nestin. A bracket marks the ventricular border. The inset shows a magnified view of SARA labeling. (C) Confocal images of dividing RG of E15.5 cortex expressing GFP (green) and labeled for endogenous SARA (red) classified according to their cleavage plane angle. DAPI is in blue. Dashed line depicts the

Development • Advance article

cleavage plane. White lines outline the borders of dividing cell pairs. (D) Percentage of GFP-labeled dividing cells with vertical cleavage plane (60°-90°), intermediate (30°-60°), and horizontal (0°-30°). (E) Mean ratios of SARA endosomal distribution between diving cell pairs classified according to their cleavage plane angle. A ratio close to 1 indicates a comparable distribution of SARA between dividing cells. Data are means ± s.e.m., P=0.58 one-way ANOVA. n= 51 cells from three brains. (F) Representative image of a GFP-expressing dividing pair (green) and labeled for endogenous Rab5 (red) at E15.5. DAPI is in blue. (G) Mean ratios of Rab5 endosomal distribution between diving cell pairs classified according their cleavage plane angle. Data are means ± s.e.m., P=0.33, one-way ANOVA. n= 21 cells from three brains. Scale bars: B= 20 µm, inset in B= 10 µm, C, F= 5 µm.

Development • Advance article

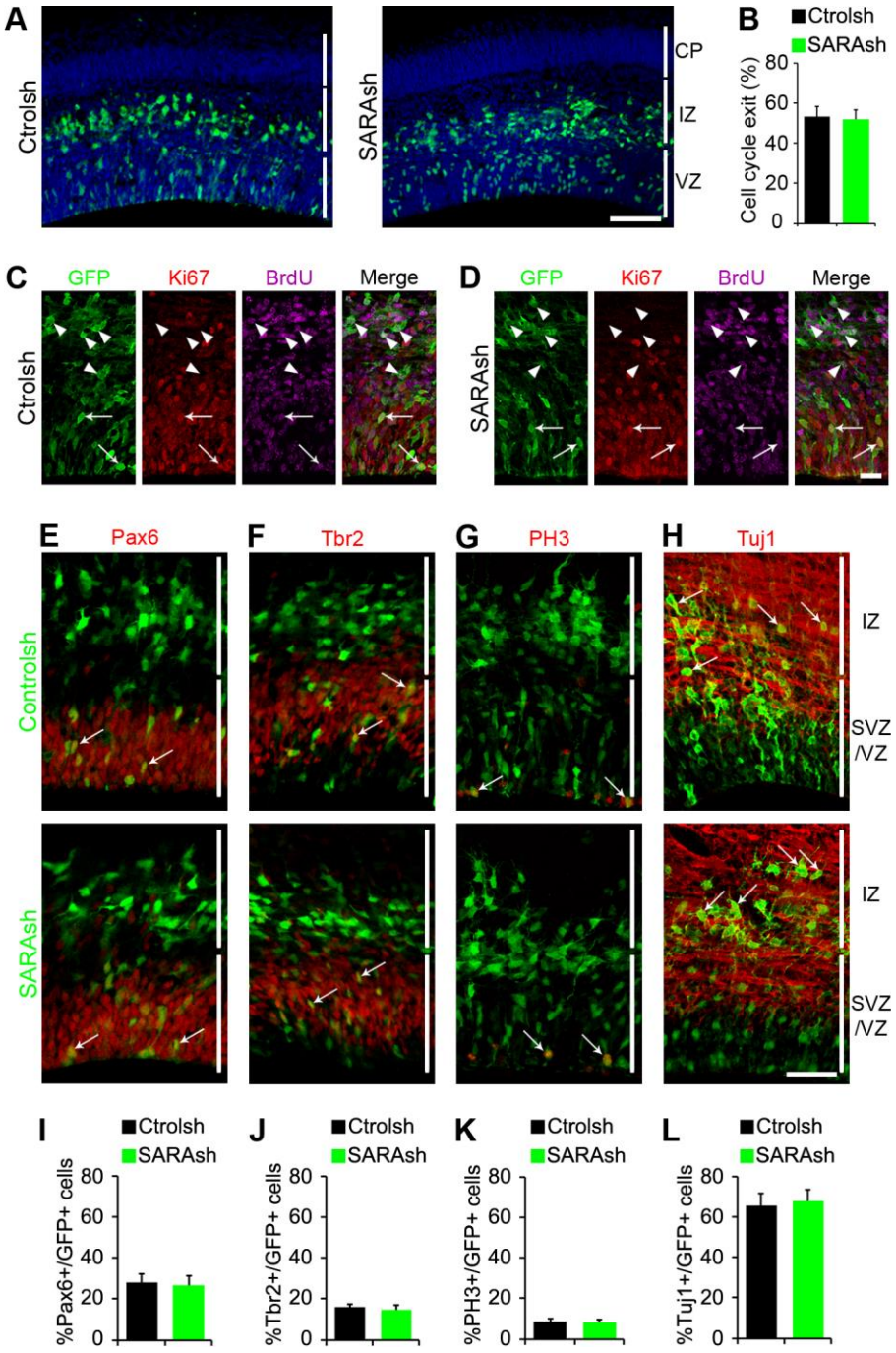

Development • Advance article

Figure 2. SARA is dispensable for neurogenesis and daughter cell fate. (A) Mouse brain slices electroporated at E13.5, either with Ctrolsh or SARAsh, and harvested 40 hours later. (B-D) Cell cycle exit analysis. (B) Percentage of GFP+, BrdU+, Ki67– cells out of total GFP+, BrdU+ cells (cell cycle exit index). Data are means ± s.e.m., P= 0.84, t-test; at least 112 cells from three brains were counted for each condition. (C-D) Representative confocal microscopy images of transfected mouse cortical slices subjected to cell cycle exit analysis. GFP+ cells (green) 24 hours after BrdU treatment (red) and stained with antibodies against Ki67 (magenta). Arrowheads point to the cells that were positive for GFP and BrdU, but negative for Ki67. Arrows point to the cells that were positive for GFP, BrdU and Ki67. (E-H) Mouse brain slices electroporated at E13.5, either with Ctrolsh or SARAsh, and harvested 40 hours later were co-labeled for Pax6, Tbr2, PH3 or Tuj1 (red). (I-L) Percentage of GFP+ transfected cells with the indicated plasmids positive for Pax6 (I), Tbr2 (J), PH3 (K) and Tuj1 (L). Data express mean ± s.e.m. At least three brains were analyzed for each condition. No significant difference was found between transfections for the indicated immunolabelings; P= 0.83 (I), P= 0.44 (J), P= 0.78 (K) and P= 0.82 (L); t-tests. Scale bars: A= 100 µm, C, D= 20 µm, E-H= 50 µm.

Development • Advance article

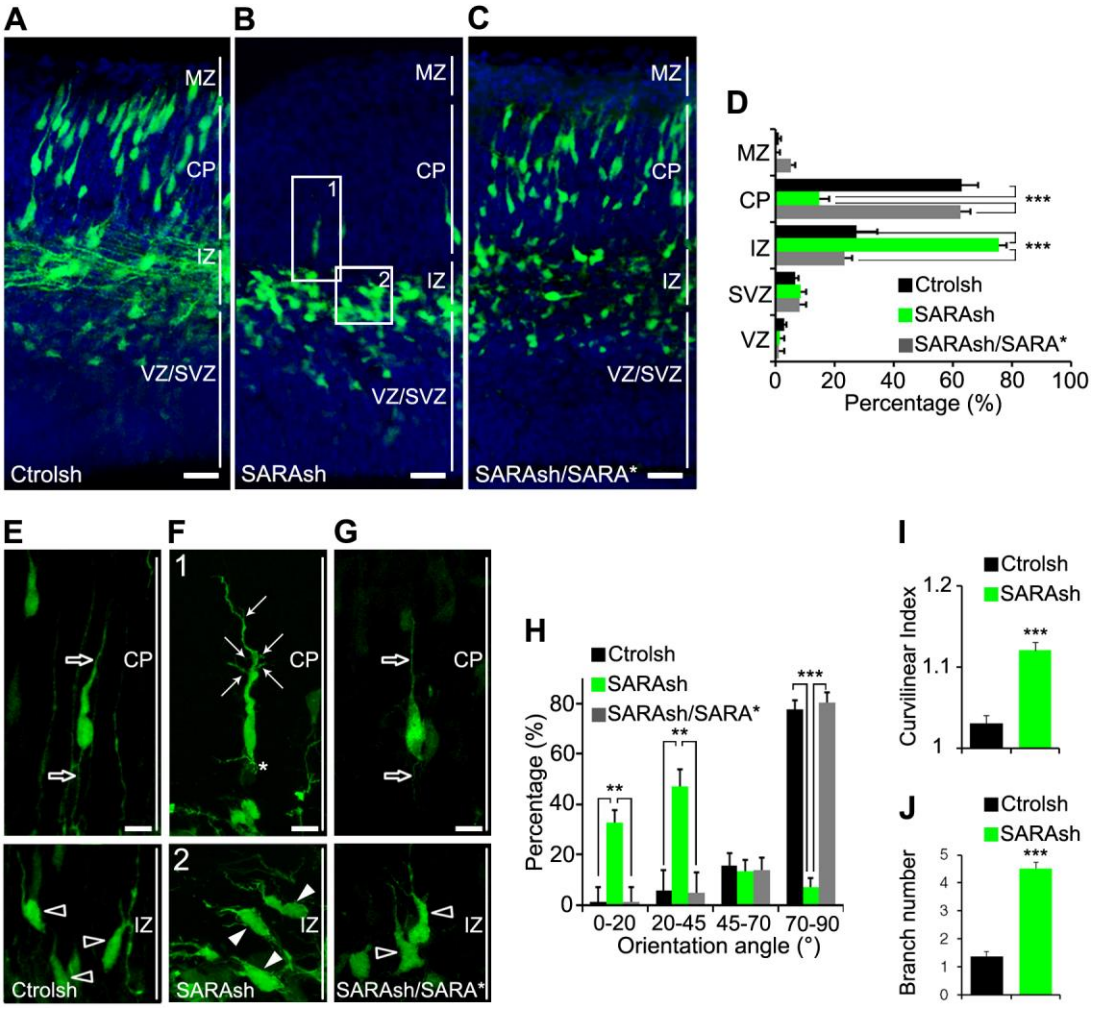

Figure 3. SARA is important for neuronal orientation and migration in developing neocortex. (A-C) Confocal micrographs of cortical slices electroporated at E13.5 with Ctrolsh (A) SARAsh (B) or SARAsh/SARA* (C) plasmids and harvested 3 days later. Blue=DAPI. SVZ: subventricular zone; MZ: marginal zone. (D) Quantification shows the percentage of transfected cells in different cortical regions with the indicated plasmids. Data are means ± s.e.m.; n, Ctrolsh= 3 brains, SARAsh= 4 brains, SARAsh/SARA*= 3 brains; *** P< 0.0001, one-way ANOVA. E-G, High power images of Ctrolsh- (E), SARAsh-transfected (F) and SARAsh/SARA*-transfected (G) neurons at the IZ and the cortical plate (CP). Open arrows (in E, G) point to single linear LP and trailing process of a control neuron at the CP. Open

arrowheads (in E, G) point to IZ-localized control neurons that typically exhibit a pia-directed orientation. (F) Shows high power images of the two boxed areas (1 and 2) in (B). Arrows and asterisk in (F) point to abnormally branched leading and trailing processes, respectively. Arrowheads in (F) point to IZ-localized SARAsh transfected neurons that had both soma and leading processes tilted from the pia-directed (vertical) angle. (H) Percentage of neurons expressing either Ctrolsh (n= 3 brains), SARAsh (n= 4 brains) or SARAsh/SARA* (n= 3 brains) classified according to their orientation angle; taking the ventricular border as the horizontal plane with an angle of 0°. For this quantification, only bipolar neurons with a clear LP, which is morphologically different from other minor processes observed in multipolar neurons, were considered. Over 300 cells were counted from at least 3 brains. Data are means ± s.e.m.; ** $P< 0.01$; *** $P< 0.0001$, one-way ANOVA. (I, J) Quantification of a curvilinear index (I) and branch number (J) for the leading processes of neurons transfected with the indicated plasmids. Data are means ± s.e.m, $P< 0.001$, t-test. Scale bars: A-C= 50 µm, E-G= 10 µm.

Development • Advance article

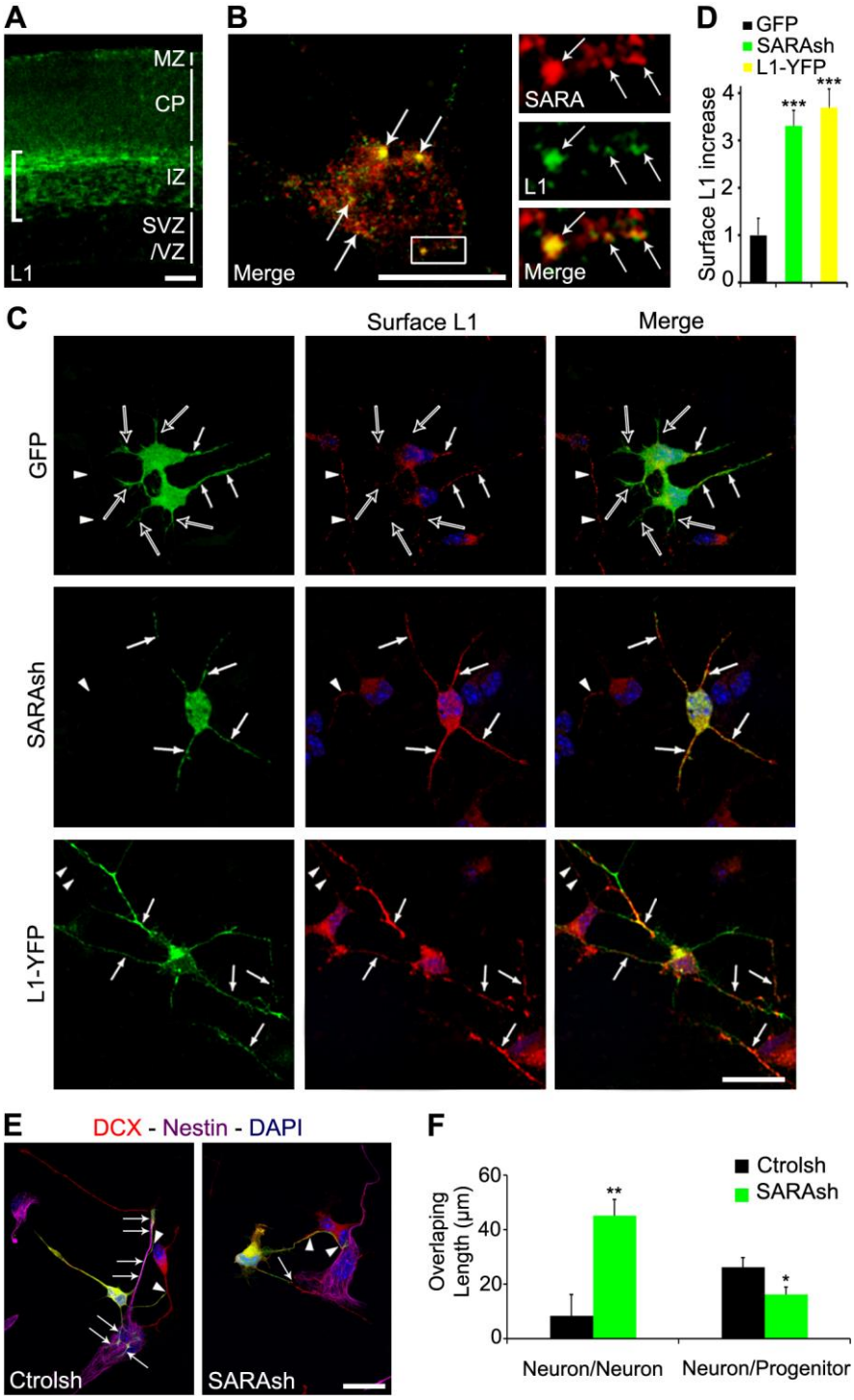

Development • Advance article

Figure 4. The cortical neuron expression of L1 and its relationship with SARA. (A) Immunolabeling of E16.5 cortical slice with endogenous L1. Bracket indicates the intense L1 signal present on the axonal tracks at the IZ. (B) Confocal images of endogenous L1 (green) and SARA (red) immunostaining of 2 DIV cultured neurons isolated from E13.5 brains. Enlarged views of a boxed area are also shown. Arrows point to the colocalization of these two molecules. (C) Cortical neurons were isolated from brains transfected with GFP, SARAsh or L1-YFP, cultured for 2 DIV, and immunolabelled for surface L1 under non-permeabilized conditions. Note that surface L1 was predominantly expressed in a single process (arrows in top panel) of GFP transfected neurons, while the remaining processes (open arrows in top panel) lacked surface L1. Stronger L1 surface signals were found in multiple processes of SARAsh and L1-YFP transfected neurons (arrows in middle and bottom panels). The surface L1 signals were much brighter than those of neighboring non-transfected GFP-negative neurons (arrowheads, middle and bottom panel). (D) Quantification of surface L1 level increase on the processes of neurons transfected with the indicated plasmids. Only neuronal processes with detectable surface L1 were scored. Data are means ± s.e.m.; *** $p<0.0001$, one-way ANOVA. At least 15 neurons from three cultures were scored for each condition. (E) Cortical dissociated cells from brains transfected either with Ctrolsh or SARAsh, cultured for 2 DIV, and immunolabelled for the neuronal marker DCX (red) and the progenitor marker Nestin (magenta). Arrows point to processes of transfected neurons growing over Nestin+ progenitor cells. Arrowheads point to neuronal processes that contact other DCX+ neurons. Under both conditions the number of neurons and glia remained similar. (F) Quantification of the overlapping length of transfected neurons on either other DCX+ neurons or Nestin+ progenitors. Data are means ± s.e.m.; * P= 0.03, ** P= 0.001, one-way ANOVA. At least 18 neurons from three cultures were scored for each condition. Scale bars: A= 35 µm, B= 5 µm, C= 10 µm, E= 20 µm.

Development • Advance article

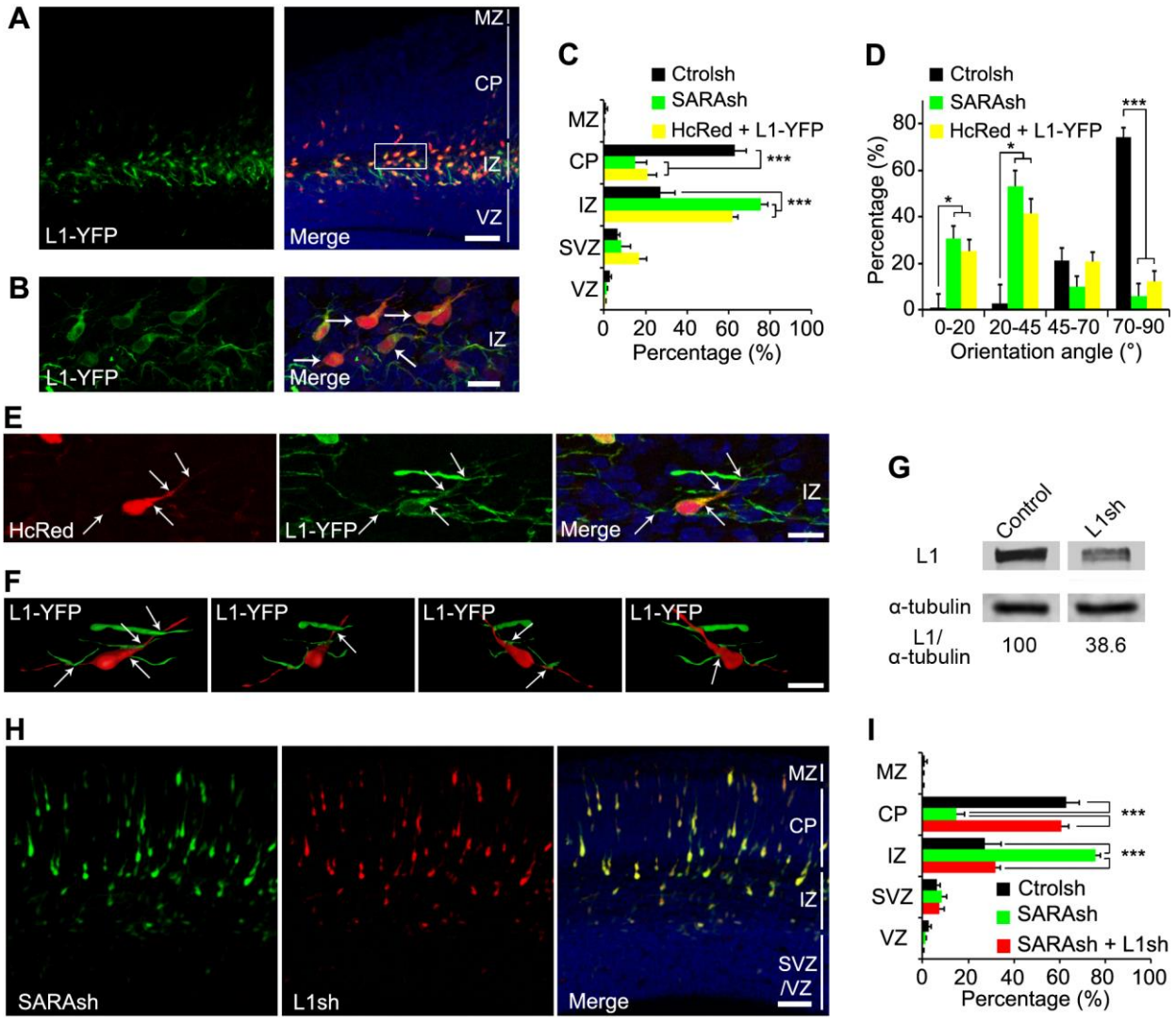

Figure 5. **Functional interaction between L1 and SARA during cortical migration.** (A, B) Cortical slices co-transfected with HcRed and L1-YFP at E13.5 and harvested 3 days later; L1-YFP was visualized by GFP immunolabeling. Higher power image of the boxed area in (A) is shown in (B). Arrows point to L1-YFP transfected neurons stalled at the IZ with a tilted orientation. (C) Quantification of the transfected cells distribution in different cortical regions. Data represent means ± s.e.m.; n, Ctrolsh= 3 brains, SARAsh= 4 brains, HcRed+L1-YFP= 6 brains; *** P<0.0001, one-way ANOVA. (D) The orientation angle of IZ and CP-localized

Development • Advance article

neurons expressing the indicated plasmids were scored by considering the ventricular border as 0°. Over 300 cells were counted from at least 3 brains. Data represent means ± s.e.m.; * P<0.05; *** p<0.0001, one-way ANOVA. (E) Shows an enlarged view of a L1-YFP/HcRed-coexpressing neuron at the IZ. Note the multiple contacts with neuronal processes from neighboring cells (arrows). Notably, L1-YFP labeled better the thin processes than HcRed. These images were rendered into a 3D reconstruction and shown in the first panel of (F). (F) Four 3D views of the IZ-localized L1-YFP transfected neuron as in (E) are shown. For simplicity, only one soma is shown; the somata of neighboring transfected cells were masked. Also see Movie 1 in which all transfected cells are shown. The cell body and its cell processes were pseudocolored in red for a better visualization of cell-neurite and neurite-neurite contact sites (arrows). (G) Validation of the silencing effect of L1sh. HEK cells were co-transfected with L1-YFP and mCherry (control) or L1sh/mCherry for 36 hours and cell lysates were processed for immunoblotting with indicated antibodies. Signal ratio of L1/α-tubulin of control is considered as 100. (H) An example of a brain slice co-transfected with SARAsh and L1sh at E13.5 and harvested 3 days later. (I) Quantification shows the percentage of cells transfected with Ctrolsh, SARAsh or SARAsh together with L1sh that distributed into different cortical regions. Data are means ± s.e.m.; n, Ctrolsh= 3 brains, SARAsh= 4 brains, SARAsh + L1sh= 4 brains; *** P<0.0001, one-way ANOVA. Note that quantifications of Ctrolsh and SARAsh transfected brains correspond to what is shown in Fig. 3, and are displayed here for comparison. Scale bar: A=50 µm, B= 12 µm, E, F= 10 µm, H= 50 µm.

Development • Advance article

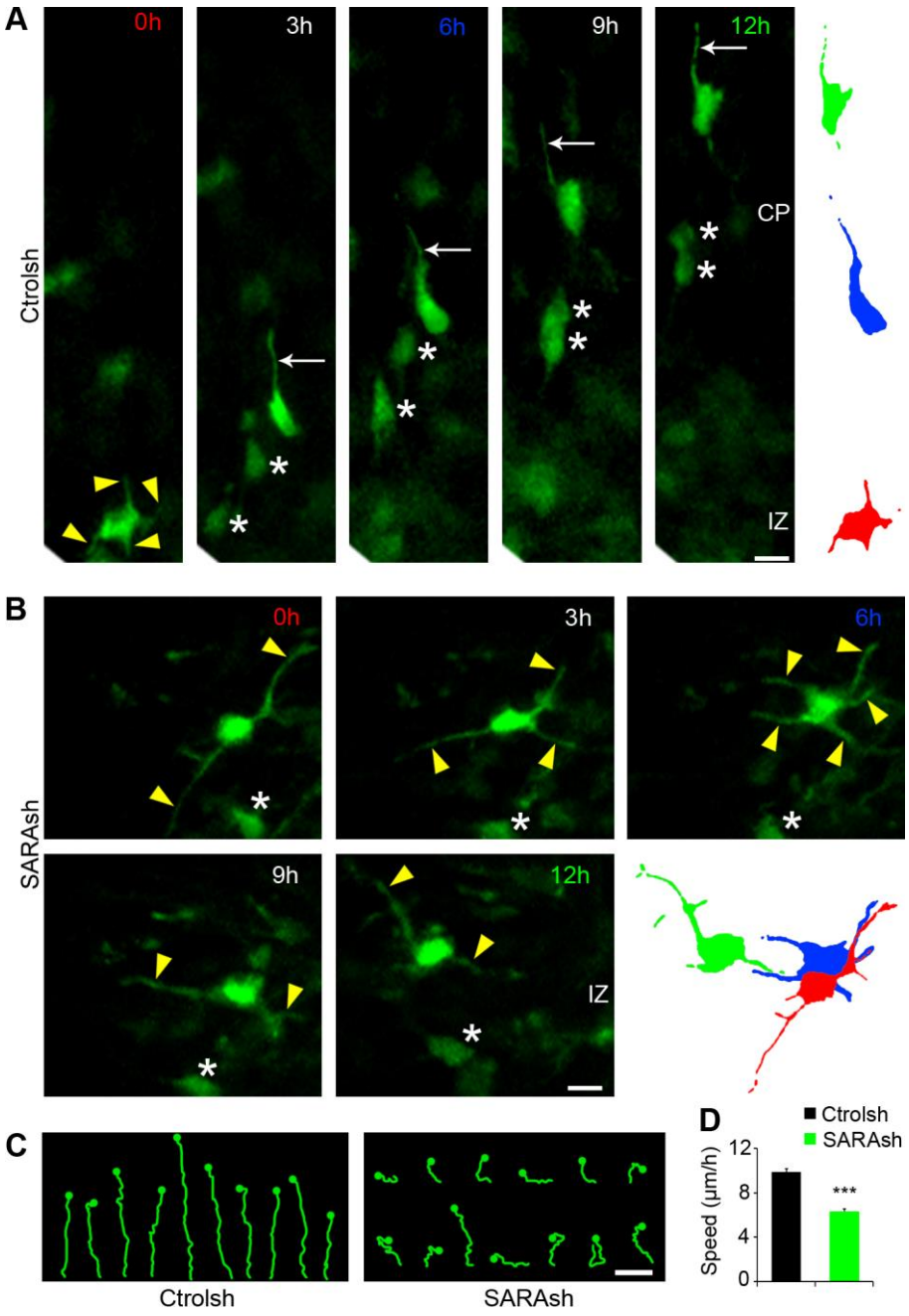

Development • Advance article

Figure 6. SARA KD cells exhibit impaired multipolar to bipolar transition. (A, B) Representative still images from time-lapse experiments tracking electroporated neurons for 12hr. Brains were electroporated with Ctrolsh or SARAsh at E13.5 and processed for slice cultures at E15.5. By the time the imaging experiment started, most neurons already localized to the SVZ/IZ. Migration trajectories and speed were evaluated from this brain area on. Yellow arrowheads point to neuronal processes of a multipolar neuron. Arrows in top panels point to the leading process of a control migrating neuron. Asterisks label the soma of other transfected neurons in the same field of view. To the right, traces represent migrating neurons at 0 h (red), 6 h (blue) and 12 h (green). In (A) a multipolar (t= 0h) Ctrolsh transfected neuron acquires a bipolar morphology and migrates into the CP. In (B) a SARAsh transfected neuron display a multipolar morphology with various processes actively extending and retracting throughout the imaged period. (C) Examples of neuron trajectories for the indicated plasmids. The dots indicate the final soma position at the end of the time-lapse experiment (t= 12h). (D) Quantification of migration speed for Ctrolsh and SARAsh transfected neurons. Data are means ± s.e.m.; P< 0.0001, t-test. At least 64 neurons were scored for each condition. Scale bar: A-C= 10 µm.

Development • Advance article

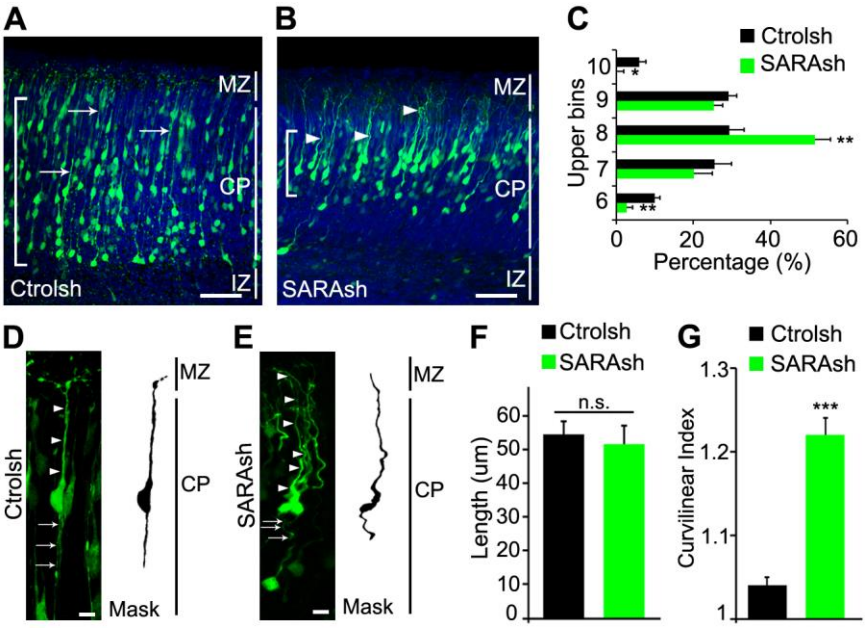

Figure 7. SARA KD cells arrive late to the CP and exhibit aberrant LP. (A-C) Mouse cortices electroporated at E13.5 with Ctrolsh (A) or SARAsh (B) plasmid and were harvested 5 days later. Control neurons have straight, linear LPs (arrows), whereas in SARAsh transfected neurons tend to be nonlinear and undulating (arrowheads). Brackets in (A) and (B) show the cortex area where most transfected cell bodies locate. Cortices were divided into 10 equally sized bins and the percentage of cells in each bin was scored; only the upper bins (6-10) contained transfected cells, and their percentages are shown in (C). Data are means ± s.e.m.; n= 3 brains for each condition; * P< 0.05, ** P< 0.001, one-way ANOVA. (D, E) High magnification images of 5-day transfected neurons. Arrowheads and arrows point to LPs and trailing processes, respectively. (F) Quantification of the LPs length of neurons transfected with the indicated plasmids. Data are means ± s.e.m.; P=0.62, t-test. (G) Quantification of a curvilinear index for the LP of neurons transfected with the indicated plasmids. Data are means ± s.e.m.; *** P< 0.0001, t-test. At least 19 neurons from three brains were scored for each condition. Scale bars: A, B= 50 µm; D, E= 10 µm.

Development • Advance article

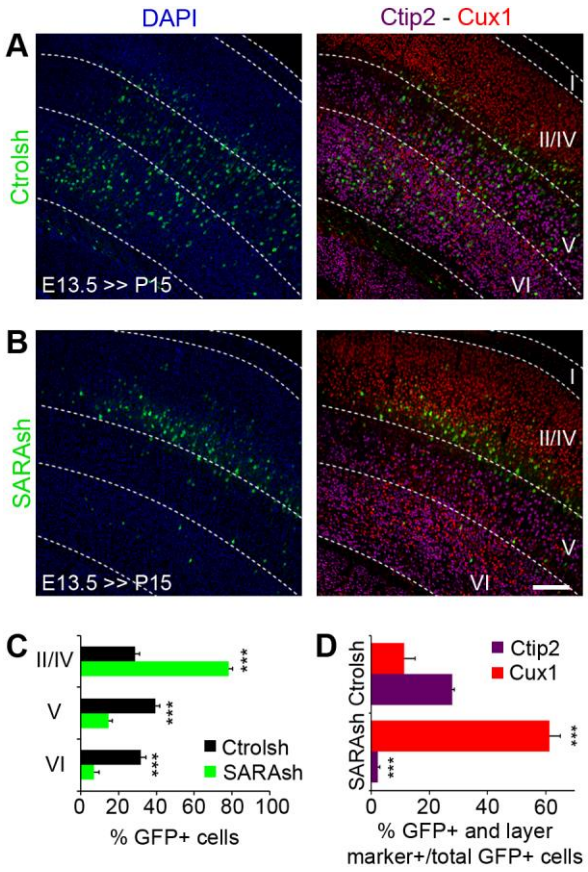

Figure 8. SARA is involved in neuronal CP positioning. (A, B) Mouse cortical slices electroporated at E13.5 with Ctrolsh (A) or SARAsh (B) plasmid and were harvested at P15 and counterstained for specific layer markers Ctip2 (magenta) and Cux1 (red). DAPI is in blue. (C) Quantification of transfected neurons with the indicated plasmids into different cortical layers. (D) Fraction of transfected cells positive for Ctip2 or Cux1 markers out of total transfected cells. Data are means ± s.e.m.; *** P< 0.0001, t-test. At least 440 cells from three brains were counted for each condition. Scale bar: A, B= 200 µm.

Development • Advance article

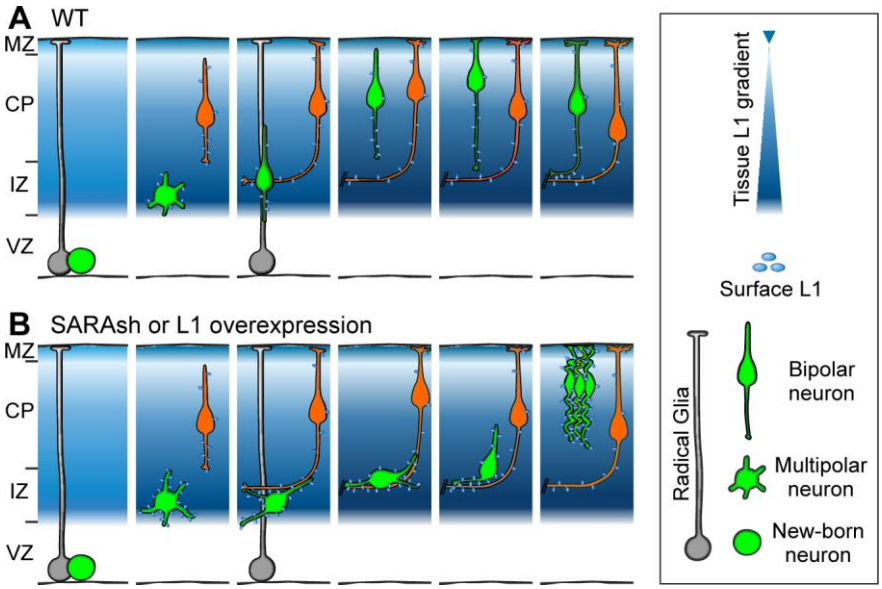

Figure 9. Schematic summary of major findings. Diagrams depict the migration of post-mitotic neurons in the developing neocortex. The blue background represents the expression level of L1. The asymmetric division of a RG gives rise to one RG (gray) with a radial process touching the pial surface, and one neuron (green) which has multipolar, and later, bipolar neurites. Intermediate basal progenitors were omitted for simplicity. (A) WT neuron undergoes radial migration through the IZ en route to the CP. (B) SARA-suppressed or L1-overexpressing migrating neurons display disorientated soma/LP, delayed multipolar-to-bipolar transition and IZ crossing. These defects are likely due to the increased surface L1 in the LPs, which forms either trans-homophilic or heterophilic (not shown) interaction with tangentially growing axons at the IZ (orange) or other migrating neurons (not shown). SARA-suppressed neurons are eventually able to overcome the IZ retention and reach the more superficial CP layers. The LPs of these neurons appear highly curved, presumably due to increased L1-mediated cell-cell and/or cell-ECM adhesion.

Development • Advance article

SARA regulates neuronal migration during neocortical development through L1 trafficking

Iván Mestres, Jen-Zen Chuang, Federico Calegari, Cecilia Conde, Ching-Hwa Sung

Supplementary Materials and Methods

Antibodies

The following antibodies were used in this study: α-tubulin mouse antibody (1:10,000, Sigma), β1 integrin rat antibody (1:100, BD Pharmingen), γ-tubulin mouse antibody (1:500, Sigma), BrdU rat antibody (1:500, Abcam), cleaved PARP rabbit antibody (1:600, Cell Signaling), Ctip2 rat antibody (1:600, Abcam), Cux1 rabbit antibody (1:300, Novus), DCX goat antibody (1:400, Santa Cruz),GFP chicken antibody (1:1,000, Abcam), Ki67 rabbit antibody (1:1000, Abcam), L1 mouse antibody (1:400, Abcam), Nestin mouse antibody (1:400, DSHB), Pax6 rabbit antibody (1:600, Covance), PH3 rat (1:600, Abcam), Rab5 rabbit antibody (1:300, Santa Cruz), RFP rabbit antibody (1:1000, Rockland), SARA rabbit antibody (1:400, Hu et al., 2002), SARA rabbit antibody (1:400, Santa Cruz), Tbr2 rabbit antibody (1:400, Abcam), Tuj1 mouse antibody (1:1000, Sigma). Various Alexa-dye conjugated secondary antibodies (1:1000, Invitrogen) and 4',6-Diamidino-2-Phenylindole, Dihydrochloride (DAPI) were also used.

DNA constructs and cell line transfection

All expression constructs were directed by CAG promoter and all sh constructs were directed by U6 promoter. The knockdown (KD) effect of SARAsh and SARAsh/SARA* have been previously validated (Chuang et al., 2007). SARAsh-IRES-GFP plasmid was generated by replacing HcRed of SARAsh-IRES-HcRed plasmid with GFP. The pCAG-L1-YFP was generated by inserting L1-YFP (a kind gift from Hiroyuki Kamiguchi [Nishimura et al., 2003]) into a pCAG vector using standard cloning method. The targeting construct of L1sh was 5’ GGGTCTCTGATCTTGAGTAACGCCATGG CGTTACTCAAGATCAGAGACCC 3’; the DNA fragment containing pU6-L1sh was inserted into pCAG-mCherry vector to generate L1sh-IRES-mCherry.

Development • Supplementary information

HEK cells were transfected using the polyethylenimine method (Li et al., 2011). Protein expression levels were estimated by immunoblotting and quantified by Odyssey Infrared scanner (LI-COR).

Imaging and quantitative analysis

All immunolabelled sections were acquired with Leica TCS SP2, Olympus FV1000 or Zeiss LSM 780 confocal microscopes, as previously described (Li et al., 2011).

To quantify the distribution of endogenous SARA or Rab5 endosomes during mitosis at the ventricle border, only dividing cell pairs were taken into account whose nuclei presented characteristic condensed segregating chromatin observed in anapahase/telophase. GFP signal was used to delimit the cells borders and normalized SARA or Rab5 fluorescence intensity was obtained for each cell with the Measure tool in ImageJ. The cleavage plane angle between the dividing pair was also scored. Finally, a ratio was calculated between the highest intensity of the two cells by the lowest.

Morphology assessment was made by considering the maximal projections images from individualized neurons to reconstruct their whole extent. In all cases, similar areas in the transfected neocortices were selected for quantification analysis.

Neurons form the upper IZ and CP were considered for orientation angle analysis. Quantification of the migration scope was carried out by dividing the cortex into its main areas: VZ, SVZ, IZ, CP and MZ; or into ten-equally sized bins; and counting the number of cells in each of these subdivisions. Measurements were normalized to cell number per slice by percentage.

Quantifications of neuronal processes mean fluorescence intensity, lengths and orientation angles were scored with the morphometric tools in ImageJ. Average background fluorescent intensity from three different empty areas in the image was subtracted to fluorescence intensity measurements over

Development • Supplementary information

neuronal processes or cell bodies. Only individually traceable neuronal processes were considered for length quantitation. Linearity index corresponds to the average ratio of total LP's length divided by the linear length from the base to the tip of the same LP. For analyzing the interaction between neurons and progenitors, the overlapping lengths of the longest neurites either with other DCX+ cells or Nestin+ cells were measured.

All images were processed using Adobe Photoshop (CS3) for presentation. Statistics was performed with Statistica software (StatSoft, v8.0). For all quantification assays, over 300 cells were counted from at least 3 brains for each condition. Image capture and analysis were done at separate times in a double-blind fashion. A t-test was designed for the comparison of two groups. One-way analysis of variance (ANOVA) was applied when more than two groups were being analyzed. A post hoc Tukey test was used for comparison between different groups. Statistical significance was defined as $P< 0.05$*, 0.01** or 0.001***.

For Movie 1, a full slice tissue 3D reconstruction and volume rendering were carried out using 94 confocal 0.4 μm-thick optical sections, with the 3D Viewer plugin in ImageJ. To highlight the contact sites in Fig. 5F, surfaces of 31 confocal sectioning planes of several individual traceable neurons and their processes were rendered; the signals from the neighboring somata and cell processes were excluded for simplicity.

Development • Supplementary information

Supplementary Figures and Movies.

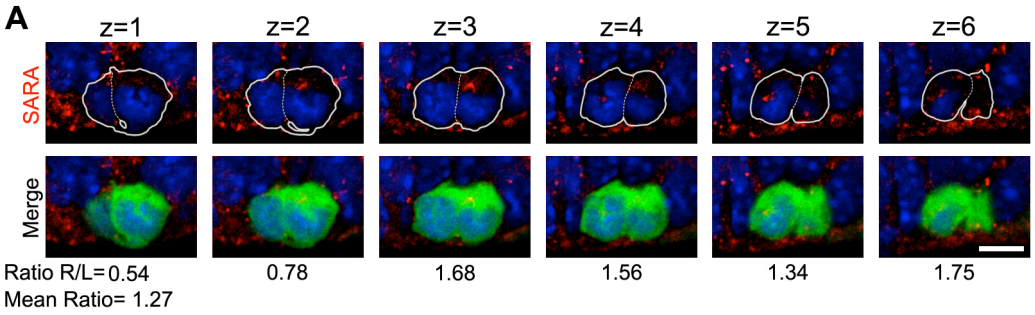

Figure S1. Related to Figure 1.

(A) Six different focal planes of a confocal z-stack showing a dividing pair of cells at the ventricle border. GFP signal delimits the cells borders. DAPI in blue shows condensed chromatin. Endogenous SARA is shown in red. Normalized SARA fluorescence intensity for each cell and plane was measured. A ratio between the fluorescence intensity of the cell to the right divided the fluorescence intensity of the left one (Ratio R/L) is provided for each z-plane. A mean ratio considering all the z-planes is also shown. Scale bar= 5 μm.

Development • Supplementary information

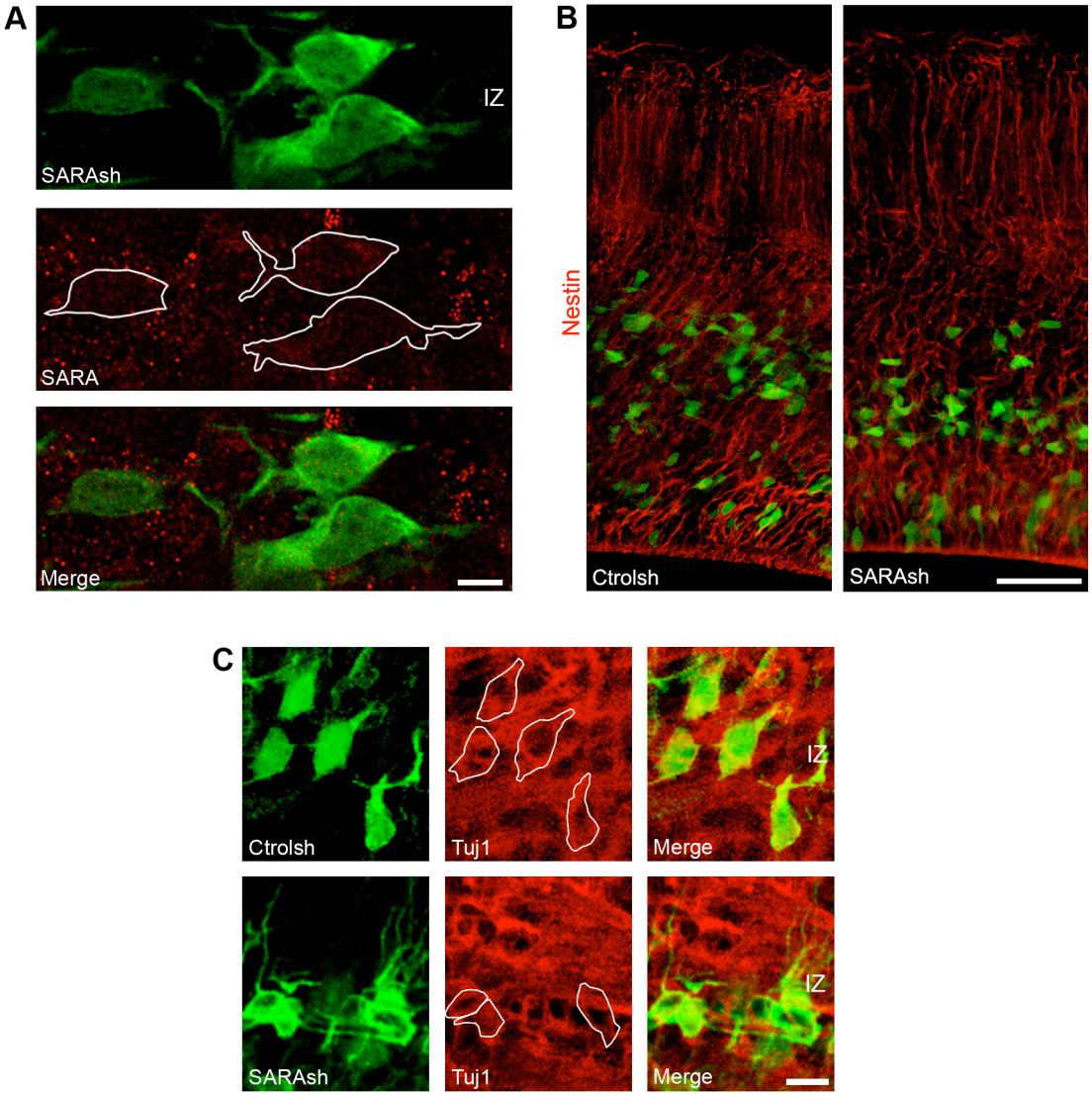

Figure S2. Related to Figure 2.

(A) Section of a mouse brain electroporated with SARAsh at E13.5, harvested 40h later and counterstained for endogenous SARA (red). Transfected cells have a decreased SARA expression compared to surrounding untransfected cells. (B) Sections of mouse brains transfected with the indicated plasmids, harvested 40h later and counterstained for the RG marker Nestin. Under both conditions progenitors processes extend radially and exhibit their apical and basal end-feet attached to the ventricle and pial borders, respectively. (C)High power images at the IZ region as in Fig. 2H. SARAsh transfected cells also expressed Tuj1, like Ctrolsh transfected cells. Scale bars A= 5 μm, B= 50 μm, C= 10 μm.

Development • Supplementary information

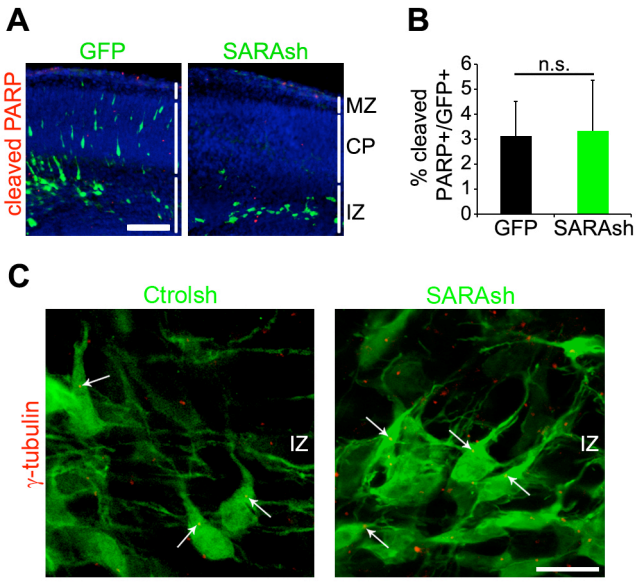

Figure S3. Related to Figure 3.

(A) Confocal images of cleaved PARP immunolabeling (red) of mouse cortical slices electroporated at E13.5 with either GFP or SARAsh for 3 days. (B) Quantification of transfected cells with the indicated plasmid positive for cleaved PARP. Data are mean ± s.e.m.; n= 4 brains for each condition. P=0.95, t-test. (C) High power images of brains sections transfected with the indicated plasmids at 13.5 and processed for counterstaining against centrosome marker γ-tubulin (arrows) 3 days later. Scale bar A= 100μm, B= 10 μm.

Development • Supplementary information

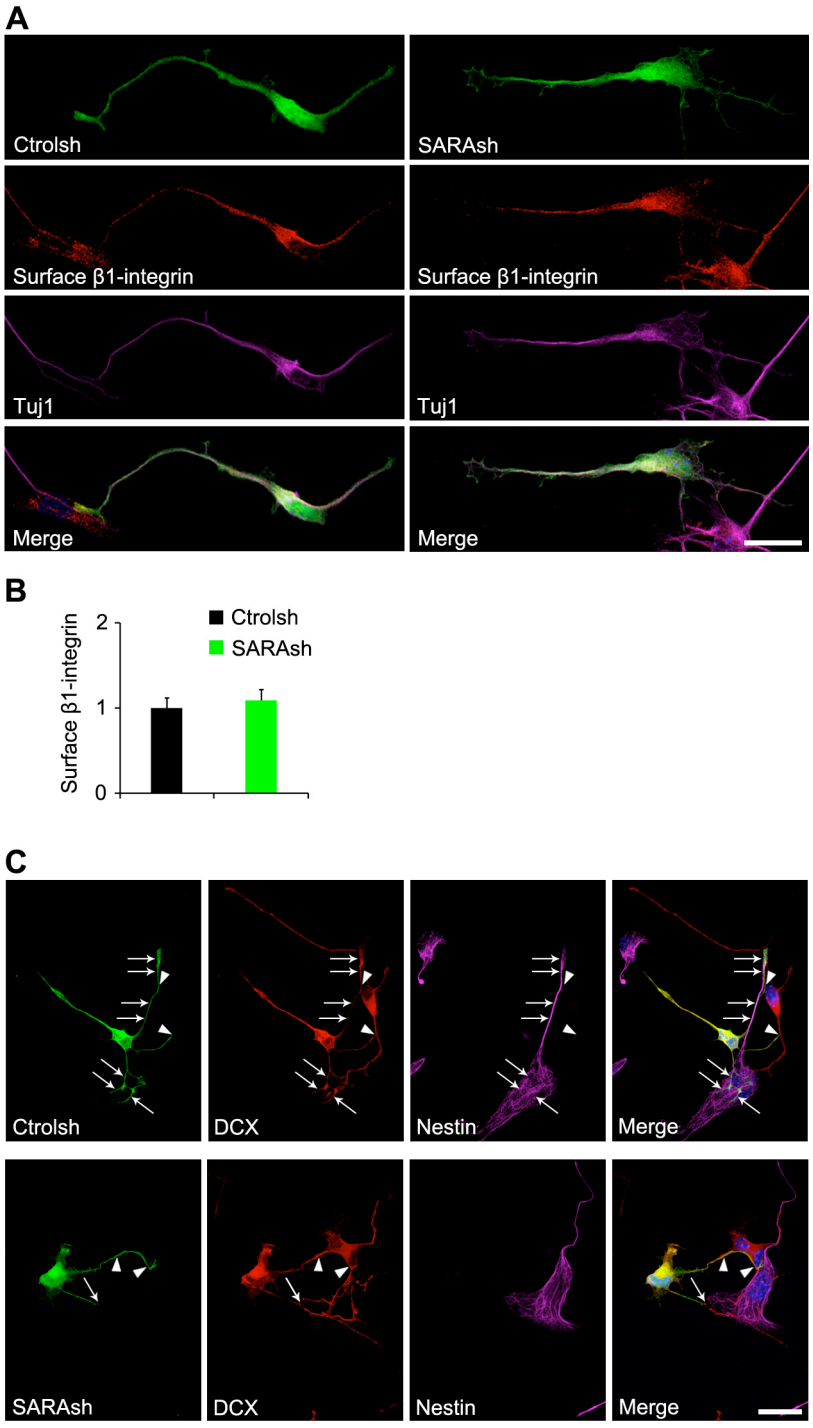

Figure S4. Related to Figure 4.
(A) Cortical neurons were isolated from brains transfected with Ctrolsh or SARAsh and cultured for 2 DIV. Cells were immunolabelled for surface β1-integrin (red) under non-permeabilized conditions. Tuj1 (magenta) staining required permeabilizing the membranes and was conducted only after incubation of primary and secondary antibodies directed to detect β1-integrin. (B) Mean fluorescence intensity of surface β1-

Development • Supplementary information

integrin on the longest neurite. Data represent mean intensity ± s.e.m., P= 0.61, t-test. At least 15 neurons were scored from three cultures for each condition. (C) Split channels of the images shown in Fig. 4E for better visualization of cell-cell contacts. Note that unlike SARA-KD neurons, Ctrolsh expressing and untransfected neurons (DCX+) preferentially extend and branch their processes over Nestin+ progenitor cells. Arrows point to processes of transfected neurons growing over Nestin+ progenitor cells. Arrowheads point to neuronal processes that contact other DCX+ neurons.
Scale bars A= 20 μm, C= 10 μm.

Development • Supplementary information

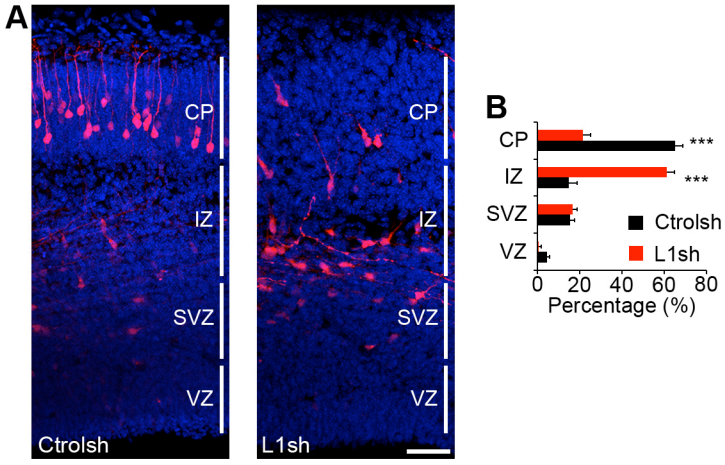

Figure S5. Related to Figure 5.
(A) Cortical slices transfected with Ctrolsh and L1sh at E13.5 and harvested 3 days later. (B) Quantification shows the percentage of transfected cells in different cortical regions with the indicated plasmids. Data are means ± s.e.m.; *** P<0.0001, one-way ANOVA. Three brains for each condition. Scale bar 50 μm.

Development • Supplementary information

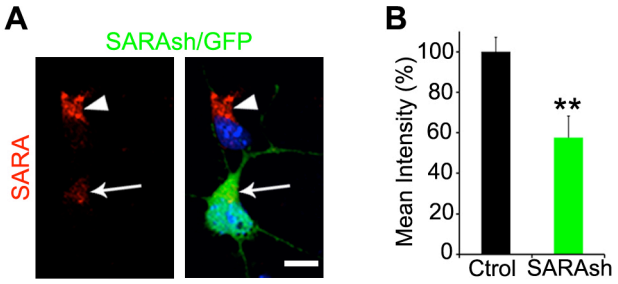

Figure S6. Related to Figure 7.

(A) Immunofluorescence of cells isolated from E13.5 brains electroporated with SARAsh and cultured in vitro for 5 days. Blue=DAPI. An arrow and arrowhead point to a transfected and an untransfected cell, respectively. Scale bar= 5 µm. (B) Quantification of immunolabeled endogenous SARA expression. Data represent mean intensity ± s.e.m.; ** P=0.0025, t-test. n= 3 independent cultures.

Development • Supplementary information

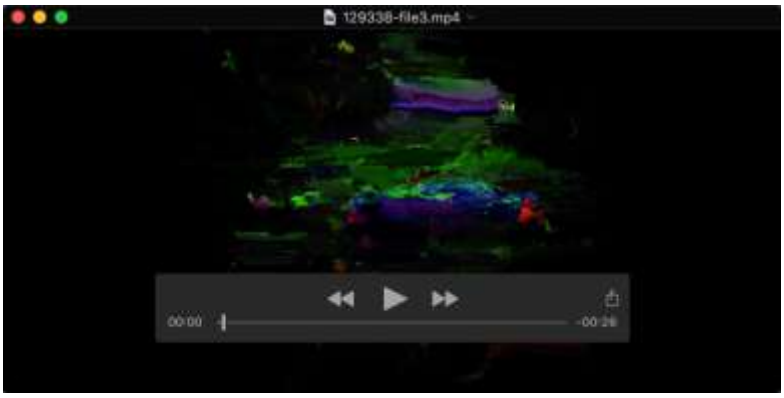

Movie 1. Full slice tissue 3D reconstruction. Related to Figure 4. Slice of a brain cotransfected with HcRed and L1-YFP. Note that several L1+ neuronal processes tangentially distributed along the IZ, coming from neurons outside the image, tangle with transfected neurons at this cortex area.

Development • Supplementary information

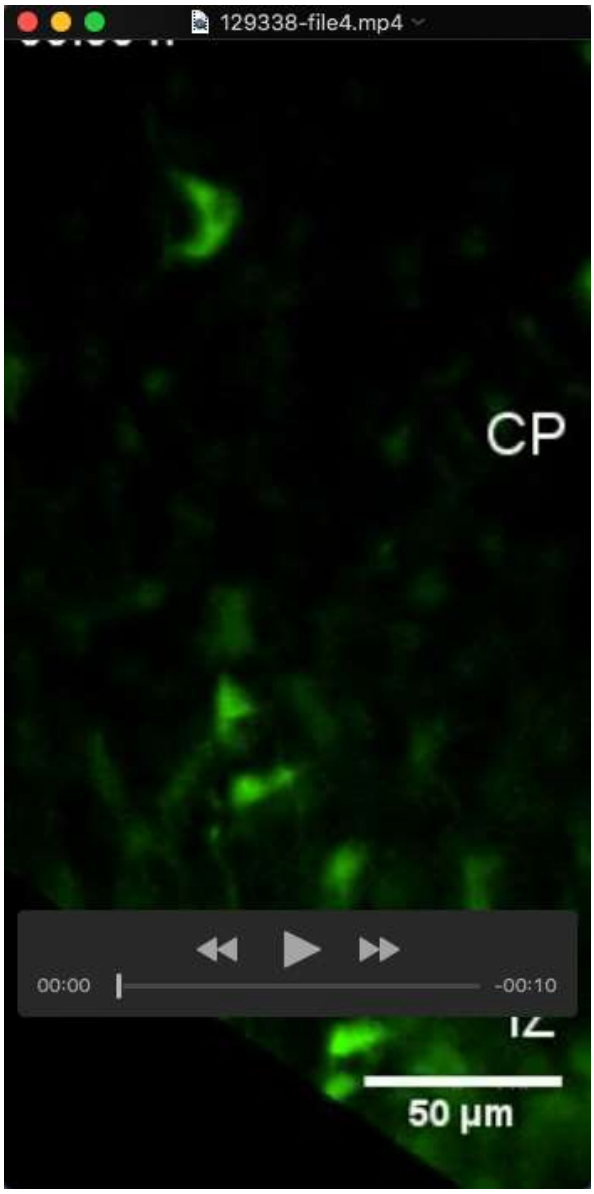

Movie 2. Related to Figure 6. Organotypic slice culture of a brain electroporated with Ctrolsh at E13.5 and processed for time-lapse imaging at E15.5 for 14 hours. Note that transfected cells exit the IZ with a vertical orientation and migrate radially towards the CP.

Development • Supplementary information

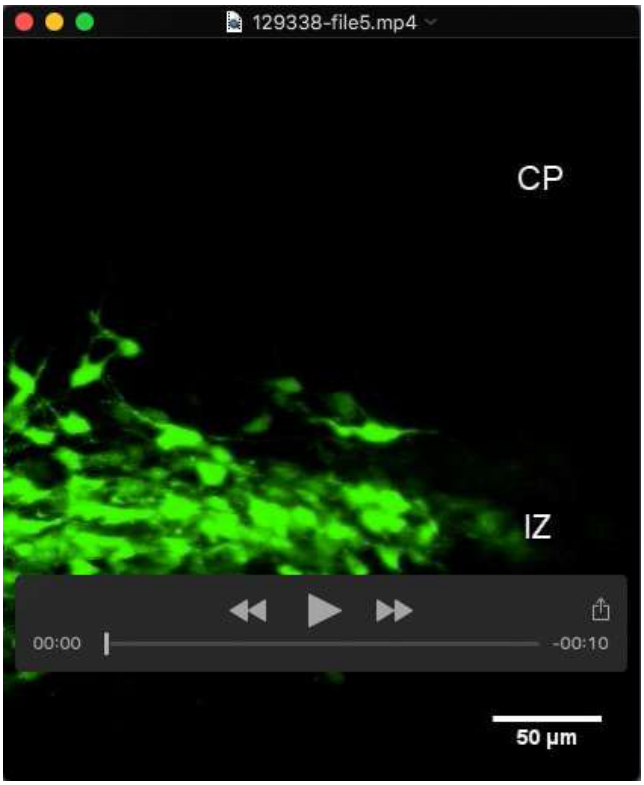

Movie 3. Related to Figure 6. Organotypic slice culture of a brain electroporated with SARAsh at E13.5 and processed for time-lapse imaging at E15.5 for 14 hours. Note that transfected cells display a tilted orientation around the IZ and are unable to migrate radially towards the CP.

Development • Supplementary information